Department of Chemistry

Stability, cation ordering and oxygen non-stoichiometry of some perovskites and related layered oxides

Matti Lehtimäki

A!

DOCTORAL DISSERTATIONS

Aalto University publication series
DOCTORAL DISSERTATIONS 118/2013

Stability, cation ordering and oxygen non-stoichiometry of some perovskites and related layered oxides

Matti Lehtimäki

Doctoral dissertation for the degree of Doctor of Science in Technology to be presented with due permission of the School of Chemical Technology for public examination and debate in Auditorium KE2 (Komppa Auditorium) at the Aalto University School of Chemical Technology (Espoo, Finland) on the 16th of August 2013 at 12 noon.

Aalto University
School of Chemical Technology
Department of Chemistry
Laboratory of Inorganic Chemistry

Supervising professor
Academy Professor Maarit Karppinen

Preliminary examiners
Dr. Christopher S. Knee, Chalmers University of Technology, Sweden
Dr. Valery Petrykin, SuperOx Japan LLC, Japan

Opponent
Dr. Michael Hayward, University of Oxford, United Kingdom

Aalto University publication series
DOCTORAL DISSERTATIONS 118/2013

ISBN 978-952-60-5263-2 (printed)
ISBN 978-952-60-5264-9 (pdf)
ISSN-L 1799-4934
ISSN 1799-4934 (printed)
ISSN 1799-4942 (pdf)
http://urn.fi/URN:ISBN:978-952-60-5264-9

Unigrafia Oy
Helsinki 2013

Finland

441 697
Printed matter

Aalto University

Abstract

Aalto University, P.O. Box 11000, FI-00076 Aalto www.aalto.fi

Author
Matti Lehtimäki

Name of the doctoral dissertation
Stability, cation ordering and oxygen non-stoichiometry of some perovskites and related layered oxides

Publisher School of Chemical Technology

Unit Department of Chemistry

Series Aalto University publication series DOCTORAL DISSERTATIONS 118/2013

Field of research Inorganic Chemistry

Manuscript submitted 8 April 2013 **Date of the defence** 16 August 2013

Permission to publish granted (date) 18 June 2013 **Language** English

☐ **Monograph** ☒ **Article dissertation (summary + original articles)**

Abstract

Perovskites and perovskite-related layered oxides have been widely studied for various applications due to their interesting physical and chemical properties. This thesis investigates the thermal stability, cation ordering and oxygen non-stoichiometry of several perovskite-related materials.

Effects of various cation substitutions on the cation ordering, thermal stability and physical properties of $Sr_2MgMoO_{6-\delta}$ double perovskite were investigated. Replacing Mg with transition metal atoms enhanced the conducting properties of the phase but depressed its thermal stability. Substitution of Mo with Nb or W retained the good thermal stability of the parent phase but the conducting properties became significantly weaker. An entirely new series of double-perovskite derived layered transition metal oxides, $(Sr_{1-x}La_x)_3(Mg_{1/3+x/2}Nb_{2/3-x/2})_2O_7$ ($0.15 \leq x \leq 0.33$), was synthesised. Like in the double perovskites, the Mg and Nb atoms were found to be ordered in these new Ruddlesden–Popper structured phases too.

Many layered transition metal oxides have been found to react with atmospheric moisture even at room temperature forming new layered compounds. In this work the effect of oxygen non-stoichiometry on the water reactivity of $A_{n+1}B_nO_{3n+1-\delta}$ Ruddlesden–Popper compounds was studied. A novel categorisation based on the crystal structure of the derivative phases was established, and the main factors affecting the reactivity were determined to be the A-site cation composition and oxygen stoichiometry of the compound.

Reversible low-temperature oxygen absorption and desorption is needed in many important applications such as three-way catalysts. The layered perovskite-derived phases, $Pb_2CuSr_2RCu_2O_{8+\delta}$, are promising oxygen-storage materials as they have been found to exhibit large oxygen absorption and desorption at relatively low temperatures. In this work it was shown that both the oxygen-storage capability and phase stability can be influenced by the selection of the rare-earth constituent R.

Keywords double perovskite, perovskite derived oxide, Ruddlesden-Popper, solid oxide fuel cell, oxygen storage, thermogravimetry, chemical substitution, phase stability, water intercalation

ISBN (printed) 978-952-60-5263-2 **ISBN (pdf)** 978-952-60-5264-9

ISSN-L 1799-4934 **ISSN (printed)** 1799-4934 **ISSN (pdf)** 1799-4942

Location of publisher Helsinki **Location of printing** Helsinki **Year** 2013

Pages 128 **urn** http://urn.fi/URN:ISBN:978-952-60-5264-9

Tekijä
Matti Lehtimäki

Väitöskirjan nimi
Joidenkin perovskiittien ja perovskiittijohdannaisten stabiilisuus, kationijärjestäytyminen ja happiepästoikiometria

Julkaisija Kemian tekniikan korkeakoulu

Yksikkö Kemian laitos

Sarja Aalto University publication series DOCTORAL DISSERTATIONS 118/2013

Tutkimusala Epäorgaaninen kemia

Käsikirjoituksen pvm 08.04.2013 **Väitöspäivä** 16.08.2013

Julkaisuluvan myöntämispäivä 18.06.2013 **Kieli** Englanti

☐ **Monografia** ☒ **Yhdistelmäväitöskirja (yhteenveto-osa + erillisartikkelit)**

Tiivistelmä

Perovskiittioksidit ja niiden kerrosrakenteiset johdannaiset ovat laajalti tutkittu yhdisteryhmä erilaisiin käyttökohteisiin monipuolisten fysikaalisten ja kemiallisten ominaisuuksiensa ansiosta. Tässä väitöskirjatyössä selvitettiin useiden perovskiittipohjaisten yhdisteiden stabiilisuutta, kationijärjestäytymistä ja happiepästoikiometriaa sekä näiden muutoksia.

Työssä tutkittiin erilaisten kationisubstituutioiden vaikutusta $Sr_2MgMoO_{6-\delta}$-kaksoisperovskiitin kiderakenteeseen, termiseen stabiilisuuteen ja fysikaalisiin ominaisuuksiin. Korvattaessa Mg-atomit siirtymämetalleilla havaittiin, että johtavuusominaisuudet parantuivat mutta terminen stabiilisuus heikentyi huomattavasti. Toisaalta Mo-atomien osittainen korvaaminen Nb- tai W-atomeilla heikensi huomattavasti johtavuusominaisuuksia mutta säilytti hyvän termisen stabiilisuuden. Lisäksi syntetisoitiin aivan uusi sarja kaksoisperovskiittien kerrosrakenteisia johdannaisia, $(Sr_{1-x}La_x)_3(Mg_{1/3+x/2}Nb_{2/3-x/2})_2O_7$ ($0.15 \leq x \leq 0.33$). Kaksoisperovskiittien tapaan näissäkin yhdisteissä Mg- ja Nb-atomien havaittiin olevan järjestäytyneinä.

Monien kerrosrakenteisten siirtymämetallioksidien on havaittu reagoivan ilmankosteuden kanssa jo huoneenlämpötilassa muodostaen uusia rakenteita. Tässä työssä selvitettiin niin sanottujen Ruddlesden–Popper-yhdisteiden, $A_{n+1}B_nO_{3n+1-\delta}$, happipitoisuuden vaikutusta yhdisteiden reaktiivisuuteen veden kanssa. Reaktiossa muodostuneille johdannaisille luotiin uusi kiderakenteeseen perustuva luokittelu ja määriteltiin tärkeimpien reaktiivisuuteen vaikuttavien tekijöiden olevan A-hilapaikan kationikoostumus sekä yhdisteen happipitoisuus.

Hapen palautuvalle absorptiolle ja desorptiolle matalissa lämpötiloissa on käyttöä monissa jokapäiväisissäkin sovelluksissa kuten katalyyteissä. Kerrosrakenteiset perovskiittijohdannaiset, $Pb_2CuSr_2RCu_2O_{8+\delta}$, ovat lupaavia hapenvarastointimateriaaleja sillä ne kykenevät absorboimaan ja desorboimaan suuria määriä happea melko alhaisissa lämpötiloissa. Tässä työssä näytettiin että sekä hapen varastointikykyyn että yhdisteen hajoamislämpötilaan voidaan vaikuttaa harvinaisen maametallin R valinnalla.

Avainsanat kaksoisperovskiitti, perovskiittijohdannainen, Ruddlesden-Popper, kiinteäoksidipolttokenno, happivarasto, termogravimetria, kemiallinen substituutio, faasin stabiilisuus, veden interkalaatio

ISBN (painettu) 978-952-60-5263-2 **ISBN (pdf)** 978-952-60-5264-9

ISSN-L 1799-4934 **ISSN (painettu)** 1799-4934 **ISSN (pdf)** 1799-4942

Julkaisupaikka Helsinki **Painopaikka** Helsinki **Vuosi** 2013

Sivumäärä 128 **urn** http://urn.fi/URN:ISBN:978-952-60-5264-9

PREFACE

The work presented in this thesis was carried out in the Laboratory of Inorganic Chemistry at Aalto University School of Chemical Technology (Helsinki University of Technology), Materials and Structures Laboratory at Tokyo Institute of Technology and Texas Materials Institute at The University of Texas at Austin between May 2006 and March 2013. Academy of Finland, The Research Foundation of Helsinki University of Technology, Emil Aaltonen Foundation and the Finnish Funding Agency for Technology and Innovation are gratefully acknowledged for the financial support of this work.

I wish to thank my instructor and supervisor Academy Professor Maarit Karppinen for the opportunity for postgraduate studies and her guidance during the years. It has been a pleasure working under her supervision. I would like to also thank Professor Hisao Yamauchi for his advice during my research and allowing me to visit Materials and Structures Laboratory at Tokyo Institute of Technology. Furthermore, I would like to thank Professor John B. Goodenough for letting me visit his laboratory at The University of Texas at Austin for a summer to broaden my research. In addition I would like to thank Dr. Yun-Hui Huang for introducing me to the world of solid oxide fuel cells during my stay in Texas. Also I would like to thank all my co-workers at the Laboratory of Inorganic Chemistry for their support.

Most importantly, I would like to thank my family and friends for their support during the years.

Espoo, July 2013

Matti Lehtimäki

CONTENTS

LIST OF PUBLICATIONS

This thesis consists of an overview and of the following publications which are referred to in the text by their Roman numerals.

I Huang, Y. H., Liang, G., Croft, M., Lehtimäki, M., Karppinen, M., Goodenough, J. B., Double-perovskite anode materials $Sr_2MMoO_{6-\delta}$ (M = Co, Ni) for solid oxide fuel cells, *Chemistry of Materials* **21**, 2319–2326 (2009).

II Vasala, S., Lehtimäki, M., Huang, Y. H., Yamauchi, H., Goodenough, J. B., Karppinen, M., Degree of order and redox balance in B-site ordered double-perovskite oxides, $Sr_2MMoO_{6-\delta}$ (M=Mg, Mn, Fe, Co, Ni, Zn), *Journal of Solid State Chemistry* **183**, 1007–1012 (2010).

III Vasala, S., Lehtimäki, M., Haw, S., Chen, J., Liu, R., Yamauchi, H., Karppinen, M., Isovalent and aliovalent substitution effects on redox chemistry of $Sr_2MgMoO_{6-\delta}$ SOFC-anode material, *Solid State Ionics* **181**, 754–759 (2010).

IV Lehtimäki, M., Yamauchi, H., Karppinen, M., Synthesis of novel Ruddlesden–Popper compounds, $(Sr_{1-x}La_x)_3(Mg_{1/3+x/2}Nb_{2/3-x/2})_2O_7$ ($0.15 \leq x \leq 0.33$), *Solid State Ionics*, **244**, 1–4 (2013).

V Matvejeff, M., Lehtimäki, M., Hirasa, A., Huang, Y.-H., Yamauchi, H., Karppinen, M., New water-containing phase derived from the $Sr_3Fe_2O_{7-\delta}$ Phase of the Ruddlesden-Popper Structure, *Chemistry of Materials* **17**, 2775–2779 (2005).

VI Lehtimäki, M., Hirasa, A., Matvejeff, M., Yamauchi, H., Karppinen, M., Water-containing derivative phases of the $Sr_{n+1}Fe_nO_{3n+1}$ series, *Journal of Solid State Chemistry* **180**, 3247–3252 (2007).

VII Lehtimäki, M., Yamauchi, H., Karppinen, M., Stability of Ruddlesden-Popper-structured oxides in humid conditions, *Journal of Solid State Chemistry*, **204**, 95–101 (2013).

VIII Lehtimäki, M., Yamauchi, H., Karppinen, M., Oxygen absorption/desorption characteristics of $Pb_2CuSr_2RCu_2O_{8+\delta}$, *Solid State Ionics* **182**, 71–75 (2011).

THE AUTHOR'S CONTRIBUTION

Publication I — The author performed the thermogravimetric measurements and analyses.

Publication II — The author defined the research plan together with co-authors. The author participated in characterization of the samples. Results were interpreted together with co-authors.

Publication III — The author defined the research plan together with co-authors. The author participated in characterization of the samples. Results were interpreted together with co-authors.

Publication IV — The author defined the research plan together with co-authors, synthesized the samples and performed all of the characterizations, except electron diffraction. Results were interpreted together with co-authors. Author had a major role in writing the manuscript.

Publication V — The author defined the research plan together with co-authors, synthesized the samples and performed most of the characterizations. Results were interpreted together with co-authors.

Publication VI — The author defined the research plan together with co-authors, synthesized the samples and performed most of the characterizations. Results were interpreted together with co-authors. Author had a major role in writing the manuscript.

Publication VII — The author defined the research plan together with co-authors, synthesized the samples and performed all of the characterizations. Results were interpreted together with co-authors. Author had a major role in writing the manuscript.

Publication VIII — The author defined the research plan together with co-authors, synthesized the samples and performed all of the characterizations. Results were interpreted together with co-authors. Author had a major role in writing the manuscript.

LIST OF ABBREVIATIONS AND SYMBOLS

ITSOFC	Intermediate temperature solid oxide fuel cell
MIEC	Mixed ionic-electronic conductor
RP	Ruddlesden-Popper
SOFC	Solid oxide fuel cell
TG	Thermogravimetry
XANES	X-ray absorption near-edge structure
XRD	X-ray diffraction

δ	Oxygen non-stoichiometry parameter
r	Ionic radius
A	Alkaline, alkaline-earth or rare-earth element
B/M	Transition metal or similar element
R	Rare-earth element
E_a	Activation energy
k_B	Boltzmann constant
σ	Electrical conductivity
S	Bragg–William long-range order parameter
g_i	Occupancy of a crystallographic site

1 INTRODUCTION

Perovskite oxides and related compounds provide us with an excellent platform for materials research with their flexible crystal structures and wide ranges of physical properties. The large variety of elemental compositions and the possibility for large amounts of oxygen vacancies allow the tuning of electrical conductivity to anything from an insulator to superconductivity[1] and magnetic properties such as ferromagnetism, antiferromagnetism and spin-glass behaviour. Among other interesting properties found in perovskites are colossal magnetoresistance,[2–4] half-metallicity[5] and multiferroic properties.[6] In addition to the aforementioned properties perovskite oxides also exhibit high oxygen-ion conductivity and catalytic activity towards the oxidation of hydrogen and hydrocarbons which can be utilised, among other applications, in solid oxide fuel cells (SOFCs). One of the currently urgent research goals is to achieve higher efficiency through the direct conversion of fuel to electricity with SOFCs, compared with internal combustion engines limited by Carnot efficiency, in non-stationary applications and distributed production of electricity. Owing to their large capability for the reversible absorption/desorption of oxygen combined with fast oxygen-diffusion kinetics, perovskites and related oxide materials may also have potential as new oxygen storage materials needed for various applications such as three-way catalysts,[7,8] gas separators[9] and oxyfuel combustion.[10]

1.1 Structure and Stoichiometry of Perovskite-Related Oxides

An ideal perovskite structure ABO_3 consists of corner-sharing BO_6 octahedra with A cations filling the empty 12-coordinated sites (Figure 1(a)). The structure can contain a large variety of different atoms with A-site atoms being usually an alkali metal, alkaline earth metal or rare-earth element and B being a transition metal or a similar element. Moreover, many perovskites are prone to accommodate large concentrations of oxygen vacancies, either ordered or randomly distributed, giving one more degree of freedom for material engineering. The wide range of possible cation compositions makes perovskite and perovskite-related materials ideal as a research subject.

A further factor affecting the perovskite structure is cation ordering. The so-called double perovskites exhibit varying degrees of cation ordering of either A- (Figure 1(b)) or B-site (Figure 1(c)) cations. The degree of order is mainly

controlled by differences in the charge, ionic radius and/or preferred coordination sphere of the cations on these sites.[11,12] The larger the differences are the higher the degree of order is. Additionally a perovskite structure can have any combination of different types of cation and anion ordering. One of the most well-known examples of such perovskites is the oxygen-deficient high-temperature superconductor $YBa_2Cu_3O_{7-\delta}$ with an ordering of both A-site cations and oxygen vacancies.[13] A partial substitution of the A site of a perovskite with very large cations may lead to an ordered perovskite where the perovskite blocks become disconnected in one lattice direction due to the preference of the large A-site cations to create a distinct layered structure (Dion–Jacobson phases[14–16]).

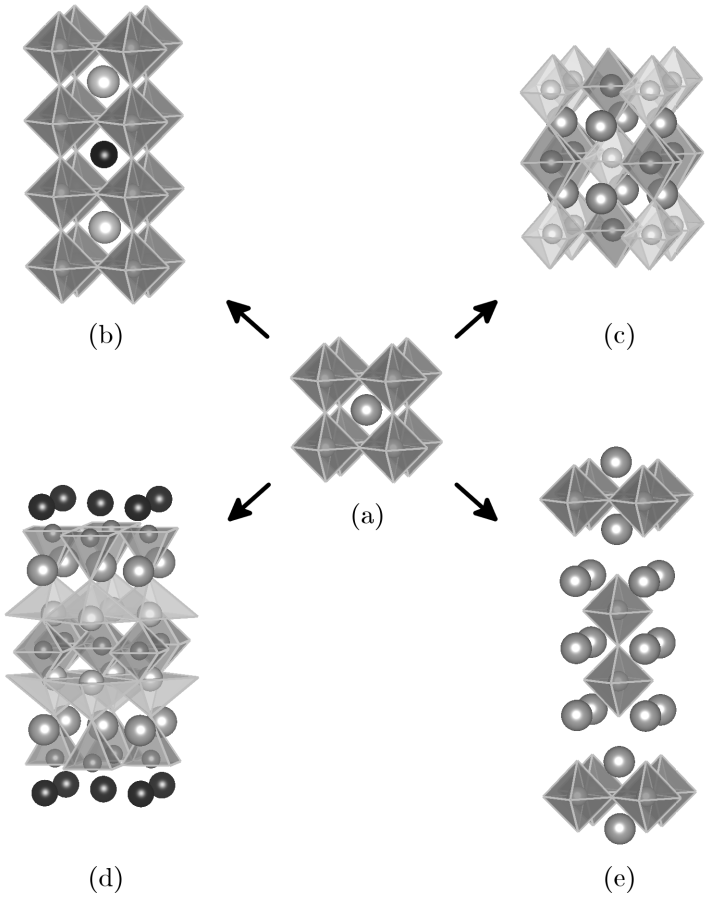

Figure 1. Crystal structures of (a) simple perovskite, (b) A-site ordered double perovskite, (c) B-site ordered double perovskite, and perovskite-derived (d) $Pb_2CuSr_2RCu_2O_{8+\delta}$ and (e) Ruddlesden–Popper phase.

The flexible perovskite structure can be even further diversified by transforming it into a layered structure by introducing one or more additional layers of different

structures between perovskite blocks. The separating layers or layer-blocks can have any of the multitude of different structures such as rock-salt (Ruddlesden–Popper phases,[17,18] Figure 1(e)), bismuth oxide (Aurivillius phases[19]), lead copper oxide (Figure 1(d)) or fluorite (many high-temperature superconductors[20–22]) type structures, and can have positive, negative or neutral charge depending on the elemental composition and the structure. The thicknesses of the individual layer-blocks and the charge distribution between them can be used to control some of the physical properties. Furthermore, some layered perovskite-related structures may, contrary to perovskites, possess oxygen excess in their structures in form of interstitial oxygen atoms.[23,24]

Occasionally the layered perovskites-related oxides, such as some Ruddlesden–Popper phases, have been found to be unstable under humid conditions and topotactically intercalate water into the structure in ambient conditions. Similar behaviour has also been observed for other types of layered compounds.[25,26]

1.2 Material Challenges of Perovskite Oxides in Applications

Perovskite oxides are used in many applications requiring high operating temperatures which may cause additional concerns in material selection. In applications such as SOFCs with operating temperatures of up to 800–1000 °C, not to mention the even higher temperatures used during manufacturing, the high temperature causes significant limitations to fuel-cell material durability.[27] The thermal stability of the compounds may result in problems since in many applications the conditions at high temperatures can be either highly oxidising or reducing thus limiting the choice of elements. Another significant limitation is caused by the aforementioned wide range of elemental compositions perovskites can exhibit. As most applications require several components to be in contact with each other, at high temperature reactions between the different components of the system become increasingly more probable and can lead to the degradation of the desired properties. In some cases, these reactions can be prevented by the introduction of a suitable buffer layer between the components but at the cost of increased complexity of the system. The high temperatures also require careful selection of the components in terms of thermal expansion which must be similar enough so that the stress on the interfaces is minimised as otherwise the stress may cause a weakening of the contact between the components or even cracking of the components. In addition to new or improved materials more optimised

manufacturing techniques can be used to improve the stability and performance of the materials. Not only is the operating temperature of application important but also the usually even higher temperatures required during the manufacturing of a system may lead to a need for improved manufacturing techniques.

The limitations caused by high operating temperatures have led to intensive research on lowering the operating temperature in applications such as fuel cells by improving the ionic and electronic conductivities and lowering interfacial resistances of the currently known materials. Moreover, new material candidates with even better physical properties and thermal stability are actively searched to achieve lower operating temperatures.

Oxygen-ion mobility is one of the key properties needed for both oxygen storage and SOFC materials, among other applications. As ionic conductivity is usually significantly, sometimes even several orders of magnitude, smaller than electronic conductivity, the careful design of the system is required to achieve high performance. In oxygen storage materials, high oxygen-ion mobility is required for reasonable kinetics during oxygen absorption/desorption. In for example SOFCs both pure oxygen-ion conductors and mixed ionic-electronic conductors (MIECs) are needed, although the latter is not imperative but is still highly desired as without MIEC elecrodes the catalytic reaction occurs only at the triple-phase boundary, *i.e.* the point where gas, electrolyte/electrode support and catalyst contact, thus rendering most of the electrode surface inactive.

Further complications may arise from minor components present in air or in other gases used in the applications. At high temperatures, the gaseous impurities become more reactive and can react with the materials used in applications or otherwise accumulate into the system due to reduction or oxidation. Not only is the stability of the materials at high temperature (both operating and manufacturing temperatures) important but also the stability of the materials at ambient conditions is of significant importance. Ambient air contains several different components which may cause problems the most common of which are water and CO_2, but also less common impurities such as oxides of nitrogen or sulphur can have significance. All of these compounds can sometimes react with oxide materials and cause the decomposition of either the surface or the whole compound through the formation of hydroxides, carbonates, nitrates or sulphates. Some perovskite-related layered oxides also have the tendency to topotactically intercalate water into the structure in ambient conditions resulting in significant expansion of the structure which may cause problems for the manufacturing and storage of the materials.

1.3 Scope of the Present Thesis

In this thesis the redox chemistry and thermal stability of some perovskites and perovskite-derived layered oxides were investigated the emphasis being on materials which could have possible uses in practical applications such as SOFCs and devices based on oxygen storage. The focus of the work was on the synthesis, phase stability, crystal structure and oxygen-stoichiometry of selected materials. The effects of isovalent and aliovalent transition metal substituents on the crystal structure, physical properties and thermal stability of *B*-site ordered double perovskites derived from $Sr_2MgMoO_{6-\delta}$ were investigated.[I,II,III] Also new Ruddlesden–Popper phases $(Sr_{1-x}La_x)_3(Mg_{1/3+x/2}Nb_{2/3-x/2})_2O_7$ ($0.15 \leq x \leq 0.33$) — related to $Sr_2MgMoO_{6-\delta}$ — were synthesised, and preliminary studies of their crystal structures were performed.[IV]

The effects of environmental and structural factors on the stability and formation of water-containing derivative phases of Ruddlesden–Popper compounds through a topotactic intercalation reaction were investigated.[V,VI,VII] A novel categorisation of the water-containing derivative phases of Ruddlesden–Popper compounds was established.[VII] Also the effect of the rare-earth element, *R*, in the perovskite-derived layered cuprate, $Pb_2CuSr_2RCu_2O_{8+\delta}$, on the rapid low-temperature oxygen absorption/desorption properties was studied.[VIII]

2 REDOX CHEMISTRY OF TRANSITION METAL OXIDES

Controlling the valence state of transition metal atoms in oxides is crucial to obtain specific functional properties whether they are electrical, magnetic, catalytic or other. Most transition metals have several stable or metastable oxidation states which can be utilised in materials design. The different oxidation states can be present in a compound either as a single oxidation state or a combination of several oxidation states, *i.e.* mixed valence. Mixed valence is often divided into three categories:[28] (i) electronically isolated crystallographically different atoms with trapped valences, (ii) valence mixing with a small activation energy of crystallographically similar atoms with distinct valences, and (iii) valence mixing of crystallographically identical atoms by delocalised electrons and equal non-integer valence.

The mixed valence of transition metal atoms in solid matter is common and can be either inherent or induced. Inverse spinel, Fe_3O_4, is an example of a compound with inherent mixed valence resulting from the stoichiometry of the compound. Another example of a compound with an inherent mixed valence is the *B*-site ordered double perovskite Sr_2FeMoO_6[5] which, contrary to Fe_3O_4, would not necessarily need to have mixed valence if simply looking at the stoichiometry of the compound. However, in Sr_2FeMoO_6, the *B*-site cations Fe and Mo are both in a mixed-valence state, II/III and VI/V, respectively due spontaneous charge transfer. Induced mixed valence can be achieved either by aliovalent substitution (*e.g.* in $(La, Sr)_2CuO_4$[29]), oxygen vacancies (*e.g.* in perovskites, $SrFeO_{3-\delta}$,[30,31] $YBa_2Cu_3O_{7-\delta}$[32,33]), cation vacancies (*e.g.* in perovskites $La_{1-x}Mn_{1-x}O_3$[34–38]), interstitial oxygen excess (*e.g.* in Ruddlesden-Popper compounds, $La_2CuO_{4+\delta}$,[23] $La_2NiO_{4+\delta}$[24]) or interstitial cation excess (*e.g.* in wurtzite compounds, $Zn_{1+x}O$[39,40]). The mixed valence of transition metal atoms makes a significant contribution to the electrical conductivity in oxides. As many of these oxides are semiconductors the mixed valence significantly improves electrical conductivity.

Controlling the oxygen non-stoichiometry of oxides is required in order to control oxide-ion conduction. A majority of the good ionic conductors have non-stoichiometry of corresponding ions as either vacancies or interstitial ions since for stoichiometric compounds operating temperatures close to their sintering temperatures are required for significant ionic conductivity.[41] Introduction of oxygen vacancies to a structure does not necessarily mean high ionic conduction

because vacancies can be trapped next to some cations, form clusters or the vacancies may become ordered with oxygen atoms. For the research of materials with purely ionic conductivity, the situation becomes even more complex since many compounds with high ionic conductivity are also electronic conductors and selection of elemental composition becomes crucial. In all compounds with high oxygen-ion conductivity, the conduction is a consequence of oxygen vacancies.[41] Changes in oxygen non-stoichiometry can sometimes be utilised directly in applications such as in oxygen storage materials. These compounds have their uses in for example catalytic converters where they are used to provide extra oxygen when needed.

Applications with high operating temperatures in highly oxidising or reducing conditions introduce new difficulties to materials design. Even though reducing/oxidation at the operating temperature is sometimes desired, excess reduction/oxidation may lead to the degradation of the desired properties or even decomposition of the phase. At operating temperatures of, for example those of conventional high-temperature SOFCs, materials are exposed to highly oxidising (cathode side) and reducing (anode side) conditions with electrolyte materials being exposed to both. Such conditions cause significant limitations to the selection of elemental composition and crystal structure for materials. Most crystal structures can include atoms in only a limited range of different oxidation states due to both introduction of either oxygen vacancies or excess oxygen and changes in cation sizes leading to decomposition, phase transition or significant changes in lattice parameters. Therefore the extreme operating conditions may in some cases prevent the usage of materials which at lower temperatures show good potential.

Investigation of redox reactions and thermal stability is commonly done by utilising thermogravimetry (TG) and other methods such as high-temperature X-ray diffraction (XRD). With TG the changes in oxygen stoichiometry can be monitored with high precision at various temperatures and atmospheres. In many applications, such as SOFCs and other applications with oxygen-ion conductors, oxygen vacancies are desired in order to obtain high oxygen mobility and electrical conductivity.

3 $Sr_2MgMoO_{6-\delta}$-BASED DOUBLE-PEROVSKITE OXIDES

Perovskite oxides have been actively researched for all parts of SOFCs. Several interesting candidates have been found for both cathode and anode materials. Most commonly used cathode material in SOFCs is the perovskite $(La, Sr)MnO_3$[42,43] which unfortunately conducts only electrons whereas several other perovskite-type cathode materials such as $(La, Sr)(Co, Fe)O_{3-\delta}$[42–44] or *A*-site ordered double perovskite $RBaCo_2O_{5+\delta}$[45–47] are of MIEC type with both electronic and ionic conduction. Several different candidates for electrolyte materials have been investigated as well, including doped cerium and bismuth oxides,[48,49] not to mention the perovskite material $La_{0.8}Sr_{0.2}Ga_{0.83}Mg_{0.17}O_{2.815}$.[50–53] Many of these materials have been found to show great potential as intermediate-temperature replacements for the most commonly used high-temperature oxide-ion conductor YSZ.

The search for new materials for SOFCs recently led to the B-site ordered double perovskite $Sr_2MgMoO_{6-\delta}$, which was found to be a promising candidate as an anode material.[54,55] It is stable in both oxidising and reducing atmospheres and highly tolerant to sulphur, which is not the case for conventional SOFC anode materials such as Ni. However, a higher concentration of H_2S still causes slight degradation of $Sr_2MgMoO_{6-\delta}$.[55] Tolerance for sulphur-containing fuels is desired as it makes using less processed natural gas and other hydrocarbon fuels possible. In addition to sulphur tolerance, $Sr_2MgMoO_{6-\delta}$ can function as a direct oxidation catalyst[54,55] and therefore reforming of hydrocarbon fuel is not necessary. Aliovalent substitution of Sr with La[56] or Sm[57] improves the fuel-cell performance and has been found to result in cation vacancies[58] in addition to the mixed valence of Mo. In the case of isovalent substitution of Sr with Ca or Ba a weak trend of increased amount of oxygen vacancies with a decreasing average ionic radius of the *A*-site cations was reported.[58]

In the present study, the effects of *B*-site substitutions of $Sr_2MgMoO_{6-\delta}$ on crystal structure, thermal stability and electrical conductivity were investigated. Substitutions on the Mg and Mo sites were done separately, for Mg selected, mostly divalent, first-row transition metals (Mn, Fe, Co, Ni, Zn) were used as substituents and for Mo the effects of both isovalent (W) and aliovalent (Nb) substitutions were investigated.

3.1 Crystal Structure

The $Sr_2MgMoO_{6-\delta}$ and its substituted derivatives are *B*-site ordered double perovskites with alternating Mo and Mg atoms on the *B* site (Figure 2). In transition metal oxides the degree of order of cations is usually described by the Bragg–William long-range order parameter,[59] defined as $S = 2g_i - 1$, where g_i is the occupancy of the cation i on its correct crystallographic site obtained from Rietveld refinement of either X-ray or neutron diffraction data. In order to fully explain the distorted crystal structure with both rotation and tilting of octahedra the triclinic space group $I\bar{1}$ has to be used.[60]

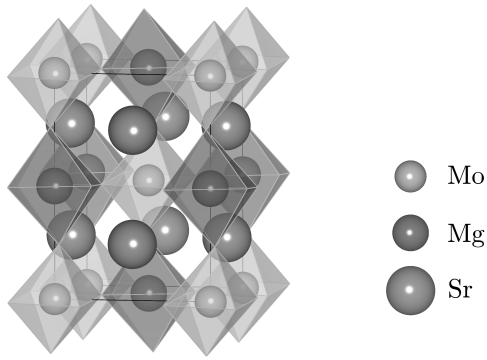

Figure 2. Crystal structure of perfectly ordered $Sr_2MgMoO_{6-\delta}$. Oxygen atoms are located at corners of the polyhedra.

In $Sr_2MgMoO_{6-\delta}$ the concentration of oxygen vacancies and the degree of order of *B*-site cations correlate strongly and can be controlled, to some degree, by the selection of a more reducing synthesis atmosphere creating more oxygen vacancies and lower degree of order.[60,II,III] The highest concentration of oxygen vacancies has been obtained when the degree of order is the lowest. This has been explained by the introduction of so-called antisite disorder which creates reducible Mo-O-Mo linkages instead of the unlikely formation of Mg^{2+} in five-coordinated form.[60] The degree of order of $Sr_2MgMo_{1-x}(Nb/W)_xO_{6-\delta}$ double perovskites decreases significantly with the substitution of Mo with Nb whereas using W as a substituent has the opposite effect and causes a slight increase in degree of order (Figure 3). This is mainly due to the smaller charge difference between Mg^{2+} and Nb^{5+} than between Mg^{2+} and Mo^{6+}/W^{6+}. Octahedral ionic radius of Nb^{5+} (0.64 Å) is also larger than that of Mo^{6+} or W^{6+}, (0.59 Å and 0.60 Å, respectively) making the difference in the ionic radius with Mg^{2+} (0.72 Å) smaller thus decreasing the tendency towards cation ordering. In addition to charge and size differences also the intrinsic oxygen vacancies, caused by the lower valence of Nb compared with

that of Mo, result in a lower degree of order by the prevention of five-coordinated Mg^{2+} as previously reported for $Sr_2MgMoO_{6-\delta}$.[60]

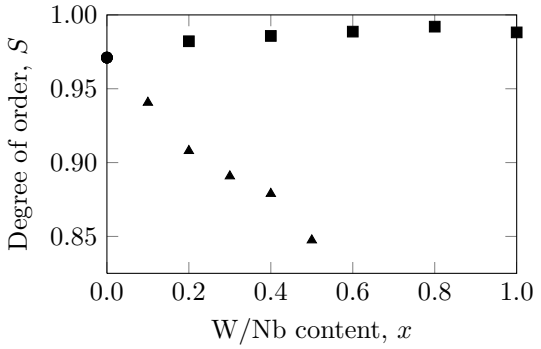

Figure 3. Dependence of the degree of order, S, of $Sr_2MgMoO_{6-\delta}$ (●), $Sr_2MgMo_{1-x}Nb_xO_{6-\delta}$ (▲) and $Sr_2MgMo_{1-x}W_xO_{6-\delta}$ (■) on the substitution level x.

Since the concentration of oxygen vacancies has a major impact on the electronic and ionic conductivities the reducibility of the air-synthesised samples of $Sr_2MgMo_{1-x}(Nb/W)_xO_{6-\delta}$ by post-annealing at 1000 °C in 5 % H_2 was investigated (Figure 4).[III] In W-substituted samples the concentration of oxygen vacancies achieved decreased with increasing substitution level, x, down to half of the value obtained for the unsubstituted compound whereas in Nb-containing samples the reducibility decreased even more rapidly with increasing amount of Nb as in the sample with $x = 0.5$ the reducibility was almost non-existent.

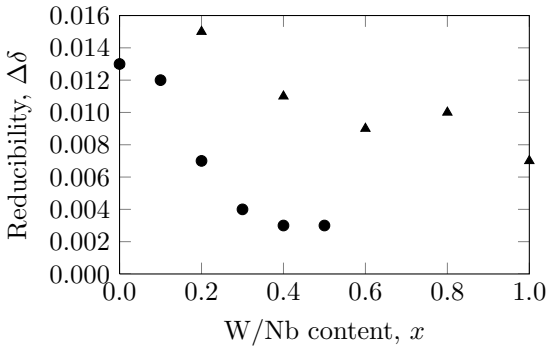

Figure 4. Dependence of the reducibility of $Sr_2MgMo_{1-x}Nb_xO_{6-\delta}$ (●) and $Sr_2MgMo_{1-x}W_xO_{6-\delta}$ (▲) at 1000°C in 5% H_2 on the substitution level x.

The lower reducibility of Nb-substituted samples may be explained by the intrinsic oxygen vacancies which hinder the formation of additional oxygen vacancies due

to the coordination chemistry of Mg^{2+} as described earlier. By utilising the X-ray absorption near-edge structure (XANES) spectroscopy measurements at Mo, Nb and W L_3- and L_2-edges it was found that in Nb-substituted samples only Nb was reduced while in W-substituted samples both Mo and W were reduced.[III] This supports the assumption that intrinsic oxygen vacancies are most likely located next to neighbouring Mo atoms and therefore fewer easily removable oxygen atoms are left in the structure. The location of the intrinsic oxygen vacancies also correlates well with the lower degree of order of Nb-containing samples.

In addition to the substitution of Mo with W and Nb, the substitution of Mg with di- or trivalent elements can be used to alter the crystal structure and properties of $Sr_2MgMoO_{6-\delta}$. Samples with $M = \mathrm{Mg, Ni, Zn}$ show a linear increase of cell volume with an increasing ionic radius of M (Figure 5) as expected for nearly fully-ordered double perovskites consisting of B-site cations only in +2 and +6 valence states.[II] On the other hand, compounds with $M = \mathrm{Mn, Fe, Co}$ show varied degrees of difference from this trend which can be explained by induction of mixed valence, or changes in the degree of order and/or oxygen non-stoichiometry. The degree of order of these compounds is significantly lowered (Figure 5), which roughly correlates with the lower unit-cell volume.[II] The lower degree of order can be explained by the mixed valence of both B-site cations, *i.e.* M^{2+}/M^{3+} and Mo^{6+}/Mo^{5+}. The lower charge difference between B-site cations and the significantly smaller ionic radius of M^{3+} than that of M^{2+}, compared with an only slight change in the ionic radius of Mo upon reduction from +6 to +5, lead to a lower degree of order.

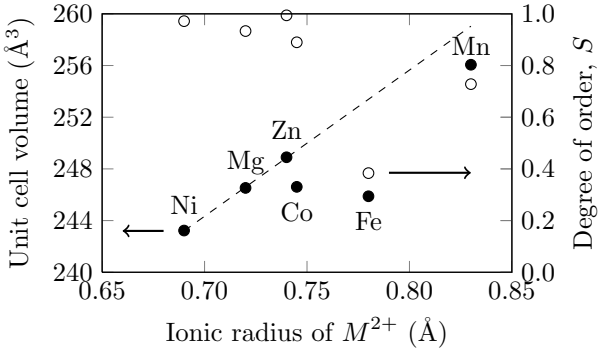

Figure 5. Unit-cell volume (•) and degree of B-site order (○) of $Sr_2MMoO_{6-\delta}$ ($M = \mathrm{Mg, Mn, Fe, Co, Ni, Zn}$) as a function of ionic radius of the transition metal constituent (M^{2+}, 6-fold coordination, high-spin state[61]). Dashed line represents the unit-cell volume trend expected for substitution with M^{2+}.

3.2 Thermal Stability

Using first-row transition metal atoms as substituents in perovskite-based anode materials has significant limitations in terms of thermal stability in potential fuel cell applications as many of these elements are easily reduced too much whereas others are easily oxidised to high valence states. If the oxidation state of transition metal in the double-perovskite structure changes too much it usually leads to at least partial decomposition of the phase. In the investigation of the thermal stability of $Sr_2MMoO_{6-\delta}$ (M = Mg, Mn, Fe, Co, Ni, Zn), significant differences were observed in thermogravimetric measurements shown in Figure 6.[II]

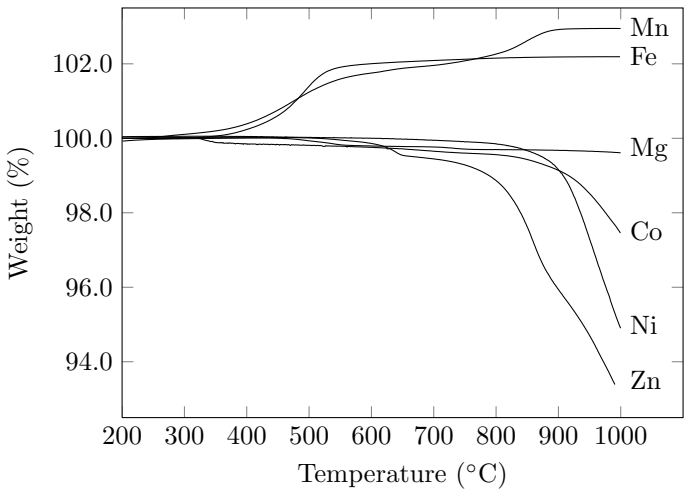

Figure 6. Behaviour of $Sr_2MMoO_{6-\delta}$ compounds at elevated temperatures. Data for M = Mn and Fe are in air, and for Mg, Co, Ni and Zn in 5% H_2.

The parent phase $Sr_2MgMoO_{6-\delta}$ is found, in agreement with previous reports,[55] to be stable in both reducing and oxidising atmospheres. The M = Mn and Fe compounds, synthesised in reducing atmospheres, are unstable in air and start to decompose above 300 °C, whereas the air-synthesised Co, Ni and Zn compounds start to decompose in reducing atmosphere at about 700, 800 and 800 °C, respectively. Compounds with M = Co or Ni can possibly be used below 800 °C[62,I,II] although somewhat larger difference between operating and decomposition temperatures would be preferable. Contrary to M = Co and Ni samples Zn substitution prevents usage at normal SOFC operating temperature of 800 °C but operation at temperature of intermediate temperature solid oxide fuel cells (ITSOFC, 500–600 °C) may be possible if catalytic properties and ionic/electrical conductivities are sufficient. Lower operating temperature is

generally needed for many types of compounds with easily reduced low-valent first-row transition metal atoms.

In contrast to the first-row transition metal atoms many of the other transition metal atoms do not exhibit as many oxidation states in oxides and are therefore much more stable in both oxidising and reducing conditions. This can be seen in the substitution of Mo with either Nb or W which do not have any significant effect on the thermal stability of $Sr_2MgMoO_{6-\delta}$.[III] The better stability is mainly due to the fact that contrary to the last first row transition metals some other transition metals (*e.g.* Ti, Mn etc.) are not so easily reduced to a metallic state.

3.3 Electrical Conductivity

In addition to thermal stability and catalytic activity also high electrical conductivity is one of the most important properties of SOFC anode materials to minimise ohmic losses, especially in the anode-supported fuel cells, which are currently the most common setup in large scale applications as the most common anode YSZ/Ni has very good electrical conductivity. Most $Sr_2MgMoO_{6-\delta}$-based compounds are mixed conductors with both electronic and ionic conduction making them potentially better than the commonly used cermet materials if their electrical conductivity can be made high enough. Usually it is said that electrical conductivity of 1 S/cm to 100 S/cm is required for electrode materials and naturally the higher the better. In electrode-supported systems higher conductivity is needed than for electrolyte-supported systems as the anode needs to be orders of magnitude thicker in the former case.

Upon substitution of Mo with either Nb or W the electrical conductivity decreases as much as several orders of magnitude as shown in Figure 7. This behaviour is somewhat expected as the substituted samples exhibit lower reducibility compared with the parent phase as stated previously. Lowered reducibility leads to fewer charge carriers and poorer electrical conductivity. The situation is, however, not so simple as there are many other factors influencing the conductivity. The poor electrical conductivities make these compounds unusable as anode materials in practical applications.

The electrical conductivities of the $Sr_2Mg(Mo, Nb/W)O_{6-\delta}$ compounds follow the small-polaron hopping mechanism[63] which has been previously reported for the parent phase.[55] In this mechanism Arrhenius' equation includes a temperature dependent pre-exponential term A/T, *i.e.* $\sigma = (A/T)e^{-E_a/k_BT}$, rather than just

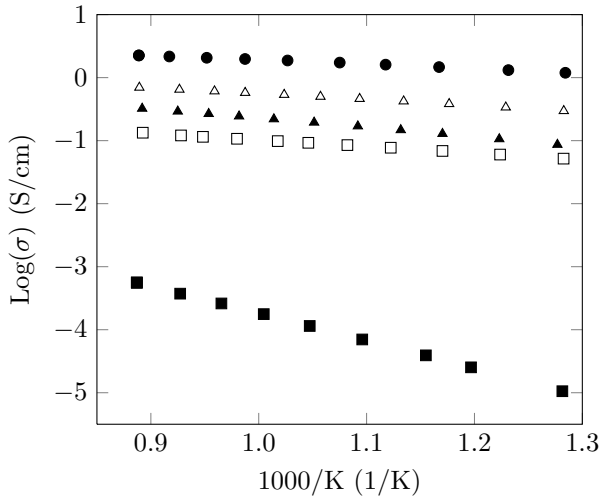

Figure 7. Temperature dependence of electrical conductivity of $Sr_2MgBO_{6-\delta}$ with B = Mo (●), $B = Mo_{0.8}Nb_{0.2}$ (△), $B = Mo_{0.5}Nb_{0.5}$ (▲), $B = Mo_{0.6}W_{0.4}$ (□) and B = W (■).

A. Activation energies obtained from a fitting of Arrhenius' equation to the conductivity data increase upon the substitution of Mo with both Nb and W.[III]

Substitution of the B-site cation Mg with di- or trivalent transition metals or other similar more easily reducible cations can be used to introduce mixed valence. Increased electrical conductivity has been observed when Mg is substituted with Co[64,65,I], Ni[62,I] and Fe.[66] All of these substituents have potential to be in either di- or trivalent state and therefore a mixed valence of Mo may result. The increased electrical conductivity in Co-substituted compounds is a result of an increase in both electronic and ionic conductivities making them even more interesting from the application point of view.[65] Small amounts of aliovalent substitution of Mg *e.g.* with Al has also been found to improve both electrical conduction and fuel-cell performance, which correlate well with increased carrier concentration.[67] The increased electrical conductivity of these compounds has also been shown to improve the power density of fuel cells in some cases.[64,65,67] In other cases such as Mn-for-Mg substitution a decreasing effect on the fuel cell performance has been seen although the electrical conductivities are similar.[55] Some of these compounds have shown varying degrees of degradation in longer measurements when using CH_4 fuel presumably due to coke formation on the anode surface.[62,66,I] Substitutions on the Mg site have also shown to be beneficial as the compounds are more easily reduced back in H_2 after potential exposure to air at the operating temperatures whereas the unsubstituted compound is

much less reduced at operating temperature. Combining both A- and B-site substitutions however has not been as beneficial since for example Ba_2MMoO_6 have been found to show lower fuel cell performance.[68]

4 RUDDLESDEN–POPPER OXIDES DERIVED FROM DOUBLE PEROVSKITES

Besides the perovskite oxides many perovskite-derived compounds such as Co-, Ni-, Cu- and Mn-based Ruddlesden–Popper (RP)[17,18] compounds have been investigated for use as a cathode material in SOFCs.[69,70] Some of these, such as the $La_2NiO_{4+\delta}$-based ones have been reported containing excess oxygen, up to $\delta = 0.25$, located in interstitial sites in the rock-salt block[24,71–73] and found to exhibit promising MIEC properties but unfortunately lower electrode performance than common perovskite materials.[74] Also RP phases related to the $Sr_2MgMoO_{6-\delta}$ double perovskite have been reported but only as an intergrowth of $Sr_2MgMoO_{6-\delta}$[75] or as a decomposition product of $Sr_2MgMoO_{6-\delta}$ under heavily reducing conditions.[60]

Ruddlesden–Popper structures consist of perovskite blocks separated by rock-salt type blocks as shown in Figure 8. These compounds have a general formula of $A_{n+1}B_nO_{3n+1}$, where A is an alkali metal, an alkaline earth metal or a rare-earth element and B is a transition metal or a similar element such as *e.g.* In, Sb or Bi. Many RP compounds possess a significant concentration of oxygen vacancies located in the centre of the perovskite block but which also affect the atomic positions in the rock-salt block.[76] Similarly to perovskites also RP compounds can exhibit B-site cation ordering.[77–84] In the present work, a novel RP phase $(Sr_{1-x}La_x)_3(Mg_{1/3+x/2}Nb_{2/3-x/2})_2O_7$ $(0.15 \leq x \leq 0.33)$ was synthesised and its thermal stability characterised.

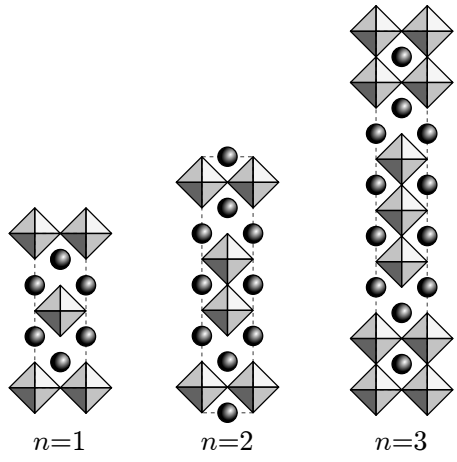

Figure 8. Structures of $A_{n+1}B_nO_{3n+1}$ Ruddlesden–Popper (RP) compounds with $n = 1, 2$ and 3.

Before the present study, RP phases in the Sr−La−Mg−Nb−O system had not been reported. Preliminary attempts to synthesise the composition closest to double perovskites, *i.e.* the $n = 2$ RP $(Sr_{1-x}La_x)_3(Mg_{0.5}Nb_{0.5})_2O_{6.5+x/2}$ ($0 \leq x \leq 1$), were mostly unsuccessful, except for the end member, $x = 0.33$.[IV] Instead of the desired compositions, a spontaneous exclusion of some SrO and MgO occurred resulting in a composition close to $(Sr_{1-\delta}La_\delta)_3(Mg_{0.5-\epsilon}Nb_{0.5+\epsilon})_2O_7$. This behaviour is most likely due to the preference of Mg^{2+} to have six-fold coordination[60] and therefore the composition became different to prevent the formation of oxygen vacancies. Based on these observations the nominal composition was altered to $(Sr_{1-x}La_x)_3(Mg_{1/3+x/2}Nb_{2/3-x/2})_2O_7$ to maintain stoichiometric oxygen content.

Most RP phases ideally crystallise in the tetragonal space group $I4/mmm$[17,18] but sometimes also in orthorhombic or monoclinic space groups. Indexing the electron diffraction (ED) data of $(Sr_{1-x}La_x)_3(Mg_{1/3+x/2}Nb_{2/3-x/2})_2O_7$ along the [0 0 1] direction (Figure 9) revealed a primitive lattice which corresponds well with the XRD data; using the $I4/mmm$ space group the XRD pattern could not be properly explained as several smaller reflections remained unexplained. Instead the orthorhombic space group ($Pmmm$; $a \approx \sqrt{2}a_I$, $b \approx \sqrt{2}a_I$, $c = c_I$) was able to explain all extra reflections. The clear supercell spots in the ED data also suggested B-site cation ordering which has been previously reported for several other RP systems.[77–84] The appearance of B-site cation ordering was somewhat expected as the charge difference is rather large and also some difference in size exists between Mg^{2+} (0.72 Å) and Nb^{5+} (0.64 Å). In many of the previous reports of B-site ordering in RP structure the ordering was only local in each perovskite block with the adjacent perovskite blocks randomly aligned and thus no long-range ordering was seen.[78–80,82,84]

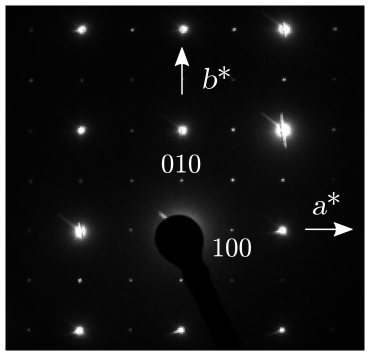

Figure 9. Electron diffraction pattern of the $x = 0.33$ sample of $(Sr_{1-x}La_x)_3(Mg_{1/3+x/2}Nb_{2/3-x/2})_2O_7$ in the [001] direction.

The profile fitting of the XRD data using the space group *Pmmm* resulted in a reasonable fit. The obtained lattice parameters decreased as the substitution level, x, increased as shown in Figure 10. The effect of substitution on the lattice parameter c is significantly larger than on a and b, both of which remaining essentially unchanged. In correspondence with the trend observed for the lattice parameters the unit-cell volume also decreases linearly with increasing x. The lattice contraction is in good agreement with the ionic radii of the substituents.

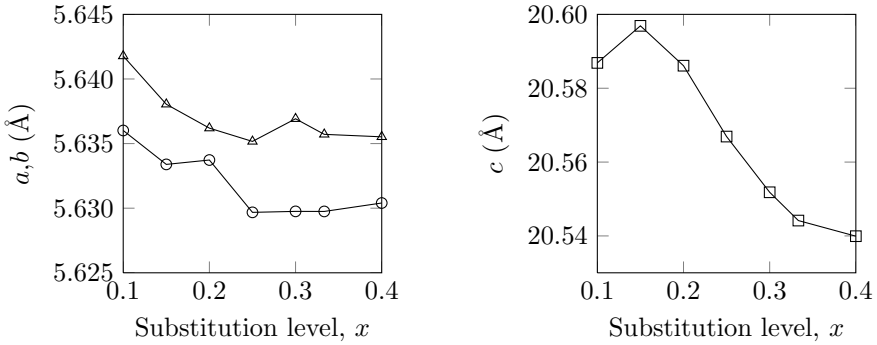

Figure 10. Dependence of the lattice parameters, a (—○—), b (—△—) and c (—□—), of $(Sr_{1-x}La_x)_3(Mg_{1/3+x/2}Nb_{2/3-x/2})_2O_7$ ($0.10 \leq x \leq 0.4$) on the substitution level, x.

Physical properties, such as electrical conductivity, of the compounds could not be determined due to poor sinterability which decreased with decreasing La content. The thermal stability of the compounds proved to be not very good since prolonged sintering at 1400 °C in air resulted in the partial decomposition of the compounds.

5 WATER INTERCALATION INTO LAYERED OXIDES

During the search for interesting properties in transition metal oxides several types of layered transition metal oxides, such as layered cobaltates,[25] Dion–Jacobson compounds[26] and Ruddlesden–Popper compounds, have been found to intercalate water as separate layers of either hydroxide or water into their crystal structure resulting in a significant expansion of the unit cell in the layer-stacking direction. Some of these have interesting properties such as superconductivity[25,85–89] and high photocatalytic activity for splitting water into hydrogen and oxygen.[90–96] In this study, the focus was chosen to be on Ruddlesden–Popper compounds due to their more versatile compositional range.

So far the intercalation of water into RP compounds has been reported for cuprates,[85–89,97–99] ferrates[100–102,V–VII], cobaltates,[102–106] indium-antimonates and -bismuthates,[81,107] titanates,[90,91,108–116] tantalates,[92,94,117–120] titanotantalates[121] and zirconates.[122,123] The large variety of different compositions for which the intercalation of water has been observed can be seen as both a positive and a negative thing. When looking for new compounds with interesting properties the wide range of elements is desirable but if the goal is to prevent the structural changes of a compound for a specific application then limitations to possible substituents are not wanted. Some cobalt- and iron-based perovskites,[42–44] for example, have been found to be reasonably promising as SOFC cathode materials and naturally it would be interesting to investigate RP compounds with similar compositions for the same application. Unfortunately the tendency of many RP compounds to react with water at room temperature is not making them very interesting materials to investigate from the application's point of view.

In the present work, the tendency of Ruddlesden–Popper compounds to react with water at ambient conditions was investigated. Particularly, the effect of oxygen content on the reactivity of these compounds was studied. A novel categorisation of the water-derivative phases into two distinctly different groups was also presented.

5.1 Water Intercalation into Iron-Based Ruddlesden–Popper Oxides

The oxygen content of the $Sr_3FeMO_{7-\delta}$ type phases has been found to influence the stability of the phase towards the intercalation of water.[V,VII] If the oxygen content is high, the intercalation is inhibited or at least too slow to be noticed in the time frame of most experiments. In the compounds which are reactive the reaction rate of intercalation increases with decreasing oxygen content.[V,VII] For samples with very low oxygen content the reaction could be observed instantly after exposing the samples to ambient conditions. In case of $Sr_3FeTiO_{7-\delta}$, the reaction was extremely slow and in order to obtain the derivative phase the sample had to be kept in a closed container with low humidity for a extended period of time.[VII] Even though the oxygen vacancies in RP structures are located in the perovskite block[76,124] they also affect the rock-salt block. The oxygen atoms coordinated with the cations of the rock-salt block are displaced towards the perovskite block to compensate the oxygen vacancies in the perovskite block and change the coordination environment of the rock-salt block cations as shown in Figure 11 based on atomic positions determined by Dann et al.[76] The altered coordination of the rock-salt block cations therefore leads to increased tendency towards water intercalation.

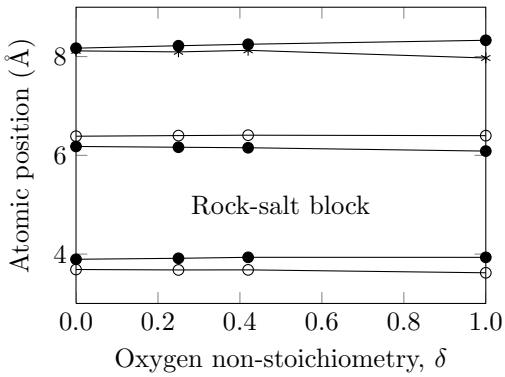

Figure 11. Coordination environment of $Sr_3Fe_2O_{7-\delta}$. Atomic symbols: Sr (—○—), Fe (—✶—) and O (—●—)

The valence of iron in $Sr_3Fe_2O_{7-\delta}$ was found, using cerimetric titrations, to become lower during the intercalation of water into the structure (Figure 12).[V] A similar reduction reaction of transition metal atoms has been observed for cuprates[88] and cobaltates/nickelates.[103,105] All of these compounds contain transition metal atoms in high valence states (Fe^{4+}, Cu^{3+}, Co^{4+}, Ni^{3+}, Ni^{4+}) which are unstable in aqueous solutions and hence the introduction of water into

the structure causes the reduction of the transition metal atoms to stable valence states.

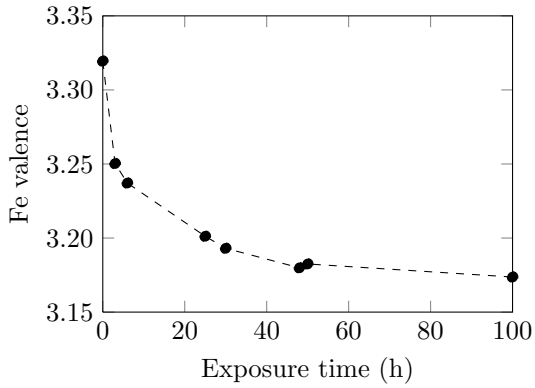

Figure 12. Time dependence of Fe valence in $Sr_3Fe_2O_{7-\delta}$ during exposure to ambient air.

The derivative phase, $Sr_3Fe_2O_{7-\delta} \cdot yH_2O$, is relatively stable under ambient conditions but upon heating the water is deintercalated from the structure in two steps and the parent phase is again obtained at approximately 250 °C as shown in Figure 13. The first plateau corresponds well with previous reports on several iron- and cobalt-based RP phases of an intermediate phase, sometimes called a hydroxide, with less water and different symmetry than the derivative phase caused by a shift of the perovskite blocks by half unit cell along [1 1 0] direction.[100,101,103–106] The intermediate phases are unstable at room temperature and additional water is reintercalated to the structure upon exposure to ambient conditions.

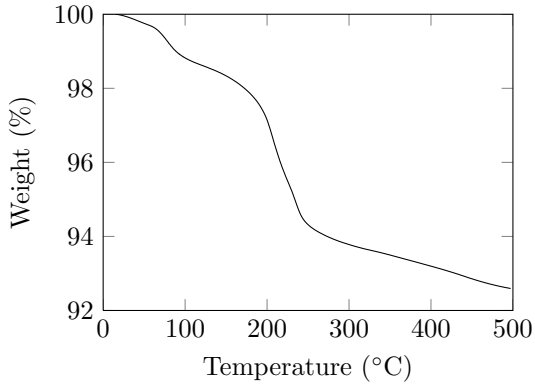

Figure 13. Deintercalation of water from $Sr_3Fe_2O_{7-\delta} \cdot yH_2O$ upon heating in air.

The intercalation of water is known to influence the physical properties of the compound by the introduction of superconductivity[25] or changes in the critical temperature.[25,85–89] Changes in magnetic properties may also occur, in $Sr_3Fe_2O_{7-\delta}$ antiferromagnetic to canted antiferromagnetic with significantly different Néel temperature as shown in Figure 14.

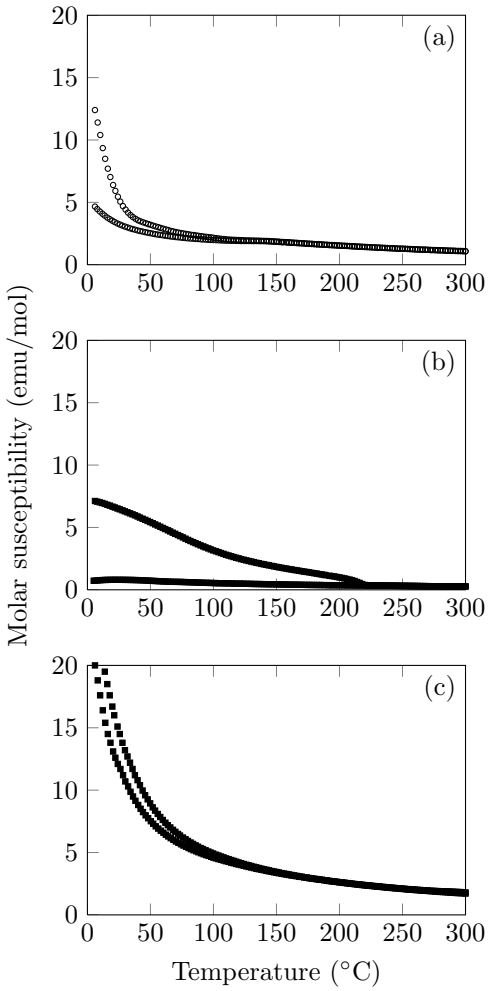

Figure 14. Magnetic behaviours of (a) $Sr_3Fe_2O_{7-\delta}$ (b) $Sr_3Fe_2O_{7-\delta} \cdot yH_2O$ and (c) $Sr_3Fe_2(OH)_{12}$.

Upon exposure to saturated humidity or submersion to deionised water at ambient temperature $Sr_3Fe_2O_{7-\delta}$ was found to form a completely different structure with the same cation stoichiometry.[V] The compound formed, $Sr_3Fe_2(OH)_{12}$ or $Sr_3Fe_2(H_4O_4)_3$, is a so-called hydrogarnet with a cubic lattice ($Ia\bar{3}d$, a = 13.2 Å).[125] Hydrogarnets are a family of minerals with a general formula of

$A_3B_2(SiO_4)_{3-x}(H_4O_4)_x$ with the end-member $A_3B_2(H_4O_4)_3$ corresponding to the compound formed in humid conditions from $Sr_3Fe_2O_{7-\delta}$.

A prolonged exposure to ambient conditions caused the decomposition of both the derivative phases and the hydrogarnet resulting in the formation of $SrCO_3$.[V–VII] As the prolonged exposure to ambient conditions sometimes causes the decomposition of the derivative phase this may result in difficulties in the detection of the water-containing derivative phases if the reaction is very slow as the newly formed phase may decompose before sufficient amounts are formed.

5.2 Water-Intercalation Reaction and Structural Changes

The effect of intercalation of water into the rock-salt block of a RP structure differs between different compounds. The water-intercalation always results in expansion of the structure in the layer-stacking, usually *c*-axis, direction to accommodate the water molecules into the rock-salt block. In addition to *c*-axis expansion the symmetry of the structure is sometimes affected, in some cases the body-centred symmetry of the parent phase (Figure 15(a)) with a staggered configuration of perovskite blocks is retained (Figure 15(b)), whereas in other there is a change in lattice symmetry from a body-centred to a primitive lattice caused by a shift of the perovskite blocks by half unit cell along the [1 1 0] direction (Figure 15(c)) leading to a so-called eclipsed configuration of perovskite blocks.

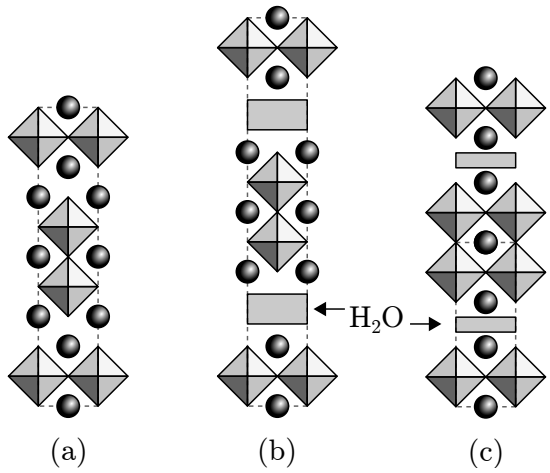

Figure 15. Schematic illustration of the crystal structures of (a) an $n = 2$ RP compound, and its (b) I-type and (c) P-type water-derivative phases.

The derivative phases can be therefore categorised into two types shown in Tables 1 and 2 according to the configuration of perovskite blocks.[VII] I-type derivative phases, with the staggered configuration of perovskite blocks, have the same symmetry as the parent RP phase. P-type derivative phases, with the eclipsed configuration of the perovskite blocks, however only have a single layer of water in their rock-salt block.

Table 1. Ruddlesden–Popper-compounds that form I-type water-containing derivative phases $A_{n+1}B_nO_{3n+1-\delta}\cdot yH_2O$. In the table Δc_w is the thickness of water layer, *i.e.* the expansion of c parameter per water block. Values marked with * are estimations.

Compound	n	Δc_w [Å]	y	Ref.
Ba_2ZrO_4	1	2.0	2.15	122
$Sr_3Zr_2O_7$	1	2.0	2	123
$Ba_2Ca_{n-1}Cu_nO_{2n+2}$	2–4	2.7–2.9	2.5–3	85–88
$Sr_2Ca_2Cu_3O_8$	3	3.0	2*	89
$Sr_{n+1}Fe_nO_{3n+1-\delta}$	1–3	3.9	2*	**V,VI**
$Sr_3FeMO_{7-\delta}$ (M = Ni, Mn, Ti)	2	3.9-4.0	2*	**VII**
$Sr_3Co_2O_{7-\delta}$	2	4.2	2*	106
$Sr_{3-\delta}Co_{1.9}Nb_{0.1}O_{6.65}$	2	4.2	1.9	103
$Sr_{n+1}(Co,Ti)_nO_{3n}$	2,3	4.2	2	104
$Sr_{2.5}La_{0.5}Co_{1.3}Ni_{0.7}O_{6.4}$	2	4.3	2*	105
$Sr_3LaFe_3O_{9.2}$	3	3.9	2	100
$Sr_3NdFe_3O_{8.5}$	3	3.4	2	101
$Sr_3PrCo_{1.5}Fe_{1.5}O_{10-\delta}$	3	3.8	2	102

Table 2. Ruddlesden–Popper-compounds that form P-type water-containing derivative phases $A_{n+1}B_nO_{3n+1-\delta}\cdot yH_2O$. In the table Δc_w is the thickness of water layer, *i.e.* the expansion of c parameter per water block. Values marked with * are estimations.

Compound	n	Δc_w [Å]	y	Ref.
$Ba_2In_{0.5}Sb_{0.5}O_4$	1			81
$Ba_2In_{0.5}Bi_{0.5}O_4$	1	2.2	3	107
Ba_3InBiO_7	2	2.1	1.7	107
$La_{2-x}Ba_xSrCu_2O_6$	2	2.3		97,98
$La_{2-x}Sr_xSrCu_2O_6$	2	2.3		99
$Na(Eu,La)TiO_4$	1	2.0	0.5–1.0	108–110
$KRTiO_4$	1	1.4–1.9	2–15	93,110,111
$A_2SrTa_2O_7$ (A = K, Rb)	2	1.9	0.9–3.6	92,94,117,118
$K_2La_{2/3}Ta_2O_7$	2	1.9	2	119
$K_2La_{3/2}Ta_3O_{10}$	3	1.9	1	96,120
$K_2(Na,Ca,Sr,La)_2(Ta,Ti)_3O_{10}$	3	2.2–2.4	0.8–10	121
$K_2R_2Ti_3O_{10}$	3	2.2–2.4	0.8–2	90,112–114
$A_2La_2(Ti,Nb)_3O_{10}$ (A = Rb, Cs)	3		0.9–3.5	91

I-type derivative phases, with the staggered configuration of perovskite blocks, have the same symmetry as the parent RP phase and their structures are often more well-defined with commonly 2 intercalated water molecules per formula unit/rock-salt block in two layers although intercalation of up to 3 water molecules per formula unit has also been reported.[85–88,122] P-type derivative phases, with the eclipsed configuration of perovskite blocks, only have a single layer of water in their rock-salt block which sometimes contains varying amounts of intercalated water molecules from less than 1[108,109] up to 15 per formula unit.[111] The large amount of water molecules in some P-type derivative phases has been explained by the formation of particle hydrates and an increase in disorder between the perovskite blocks.[113]

Whether the symmetry of the RP phase changes in the intercalation reaction can be in most cases determined from the chemical composition of the parent phase. If the cation in the rock-salt block is an alkaline earth metal, *e.g.* Sr, the symmetry of the parent phase is retained and the compound can be categorised as I-type, whereas if the rock-salt block consists of alkali metals, *e.g.* Na, K, Rb or Cs, the symmetry changes resulting in categorisation as P-type derivative phase. Derivative phases with the large alkaline earth metal Ba in their rock-salt block are borderline cases and can exhibit either type of symmetry.

The amount of *c*-axis expansion differs between the I- and P-type derivative phases with I-type phases having mostly larger expansion. The *c*-axis expansion of compounds with Ba in the rock-salt block is a borderline case the same way as they are in the case of changes in symmetry.

The derivative phases of RP compounds resulting from the intercalation of water are not thermally very stable. Upon heating above room temperature the intercalated water molecules are easily deintercalated and structural changes occur. I-type derivative phases often deintercalate water in two distinct steps, first of which is typically at around 50–100 °C and the second at 200–300 °C; usually half of the intercalated water is removed at each step. After the first step the structure resembles that of a P-type derivative phase with a primitive symmetry[101,104,106] with perovskite blocks in an eclipsed configuration compared with the staggered configuration in both the parent phase and the I-type derivative phase.

The water in P-type phases can deintercalate in a single step[114,120] or in two distinct steps[108,118,119] depending on the number of intercalated water molecules and crystal structure. The poor thermal stability of the derivative phases limits the use of these materials in applications where elevated temperatures are used.

However, special low temperature applications may still be possible, although the sintered pellets of parent RP become powder after 12 h exposure to air[101,104,106] making them even less suitable for many applications.

The form which the intercalated water takes in the structure is controversial because determining the positions of light elements, especially hydrogen, of water is not easy due to reasonably low scattering with both X-rays and neutrons. A reasonable model for the positions of oxygen atoms in both the derivative and intermediate phases has been reported.[101,104,106] The model for the derivative phase consists of a double-layer of water with transition metal octahedra adjacent to the rock-salt block becoming square pyramids as oxygen atoms of the rock-salt layers move towards the water layers. The model for the intermediate phase is essentially the same but with only a single water layer in the rock-salt block. In neither of these models, the positions of hydrogen atoms are reported.

Similarly to the case observed for the iron-based RP compounds[V,VII], the reduction of the very high oxidation states of transition metal atoms in the structure is observed also with for example copper[88] and cobalt/nickel[105] based compounds. As the transition metal is reduced some element has to be oxidised. Most probable reactions are the oxidation of oxide ions to elemental oxygen (Reaction 1) or the formation of peroxide bonds (Reaction 2). In the former of these reactions, the resultant protons form either hydroxide- (Reaction 3) or oxonium-ions (Reaction 4). Whether the oxidised oxide ions are from the intercalated water or from the original lattice is yet to be determined.

$$4B^{z+1} + 2\,H_2O \longrightarrow 4B^{z} + 4H^{+} + O_2\uparrow \quad (1)$$

$$2B^{z+1} + 2\,O^{2-} \longrightarrow 2B^{z} + O_2^{2-} \quad (2)$$

$$H^{+} + O^{2-} \longrightarrow OH^{-} \quad (3)$$

$$H^{+} + H_2O \longrightarrow H_3O^{+} \quad (4)$$

5.3 Reactivity of Ruddlesden–Popper Oxides

Not all Ruddlesden–Popper compounds react with water under ambient conditions and not even after immersion in water for extended periods of time, whereas some react immediately after exposure to ambient air. In fact it is assumed that most RP compounds are stable under ambient conditions although it may also be that many reactive RP compounds are yet to be found possibly due to their slow

reaction rates or unsuitable oxygen contents. In some cases if the reaction is slow enough and the derivative phase unstable it may be impossible to observe the derivative phase as the amount of it would always be below the detection limits of usual analysis methods such as XRD whereas thermogravimetry, for example, is more suitable for the detection water intercalation.

The elemental composition of an RP compound has a significant effect on the stability and atoms with the biggest influence are the cations present in the rock-salt block. If the majority of cations in the rock-salt block are large cations, *e.g.* Ba, K, Rb or Cs, then the compounds have a higher tendency for the intercalation of water into the rock-salt block. In the normal coordination, a cation in the rock-salt block has 9 neighbouring oxygen atoms. Therefore the preferred coordination sphere of the atoms has a major role in determining the reactivity of the compound with larger cations which usually tend to prefer higher coordination numbers. Despite the presence of suitable cations in the rock-salt block not all such compounds react with water even after prolonged exposure to humid conditions or immersion in water. Substitution of A site with smaller alkali metals or alkaline earth metals such as Na[126,127] or Ca may inhibit the reaction with water. When replacing A cations with the smallest alkali metal Li, the structure of the block separating perovskite blocks is no longer of rock-salt type but a single layer of tetrahedrally coordinated LiO is formed instead. Even though the staggered configuration of adjacent perovskite blocks remains, due to the very small interlayer distance in these compounds they do not form derivative phases.[114,128,129] Also rare earth elements as substituents have been found to increase the stability of the parent RP phase as in for example P-type phases the rock-salt blocks with only rare-earth elements do not react with water, which is easily observable in $n = 1$ RP compounds with alkali-metal and rare-earth atoms ordered into alternating rock-salt blocks.[108,109,111] On the other hand I-type phases with some amount of rare-earth substituents with alkaline earth metals have been found to react with water[100,101,105] although these compounds still have a majority of alkaline earth metal atoms in their rock-salt blocks. It has also been reported that B-site substitution of Ti with Zr can stabilise even K-containing compounds.[93]

Introduction of oxygen vacancies, formed into the perovskite block, to a RP structure causes a shift of oxygen atoms of the rock-salt block towards the perovskite block[76,124] and therefore the oxygen content of an RP compound is also a major affecting factor on the reactivity of an RP phase but mostly in compounds with smaller and divalent cations in the rock-salt block which do not react with water when nearly stoichiometric, however after reduction reactivity

can be achieved.[100] Introduction of more oxygen vacancies to an RP compound increases the rate of transformation to I-type derivative phases significantly with clear signs of a derivative phase visible in XRD pattern already after less than an hour of exposure to ambient air whereas the same compound with a higher oxygen content does not show any signs of the derivative-phase formation after several hours of exposure.[V,VII] However, the influence of oxygen content is not as simple since it has been reported that too low an oxygen content can also prevent the water intercalation into the structure.[102]

Instead of the possible applications of the derivative phases at least equally interesting is the effect of the derivative-phase formation on the usability of the parent RP compounds themselves. Using RP compounds in practical applications usually requires stability in ambient air if not during the actual operation then preferably at least during manufacturing, storage and possible maintenance. This poses a problem for RP compounds susceptible to the intercalation of water making them unsuitable for many applications. By careful selection of substituents, the instability of these compounds may be avoided but possibly at the expence of some properties.

6 OXYGEN ABSORPTION/DESORPTION IN LAYERED $Pb_2CuSr_2RCu_2O_{8+\delta}$ OXIDES

Efficient oxygen storage materials capable of reversibly store and release large amounts of oxygen under mild conditions are highly demanded for a variety of industrial applications. The presently existing oxygen storage materials are already used as three-way catalysts in automobiles for cleaning exhaust gases.[7,8] Moreover envisaged are applications for H_2-O_2 fuel cells, oxyfuel combustion, oxygen separators, hydrogen production through solar water splitting, various non-aerobic oxidation processes, etc.[9,10,130–132] Recently $YBaCo_4O_{7+\delta}$[133] and its cation-substituted derivatives[134–139] have been under active research for their promising low-temperature oxygen absorption/desorption capability. These compounds having a rapid oxygen absorption/desorption at low temperature usually also have high oxygen mobility which can be utilised in for example ITSOFCs.[139–141] Due to recent increasing interest in $YBaCo_4O_{7+\delta}$-based compounds for various applications, the $Pb_2CuSr_2RCu_2O_{8+\delta}$ (R = La, Nd, Eu, Y, Er, Yb, Lu) series was revisited in the present thesis for a systematic evaluation of the effect of the rare-earth constituent R on the similar low-temperature oxygen absorption/desorption behaviour and high-temperature stability.[VIII]

6.1 Crystal Structure

The layered $Pb_2CuSr_2RCu_2O_{8+\delta}$ compounds (Figure 16) consist of inherently oxygen-deficient perovskite blocks — with copper in square-pyramidal coordination — separated by a [PbO]–[CuO_δ]–[PbO] block.[142–144] In the oxygen-stoichiometric compounds, $\delta = 0$, the separating block contains O–Cu–O chains along the c-axis direction between the PbO layers consisting of edge-shared square-pyramids. The copper atoms in the perovskite block are divalent whereas the Cu and Pb in the separating block are monovalent and divalent, respectively, due to coordination environment.[145–147] Upon full oxygen intake, $\delta = 2$, both copper and lead in the separating block are oxidised to +II and mixed +III/+IV, respectively. The coordination of the Cu atoms in the separating block becomes octahedral and Pb atoms end up in nine-fold coordination. The lattice of the fully-oxidised compounds, $Pb_2CuSr_2RCu_2O_{10}$, has been found to be tetragonal instead of orthorhombic observed for the oxygen-deficient phase.[143] The non-oxidised phases, $\delta = 0$, were initially investigated for their superconducting properties present after hole doping, *i.e.* the partial oxidation of Cu^{2+} in the perovskite block to Cu^{3+}, by partial Ca-for-R substitution.[142]

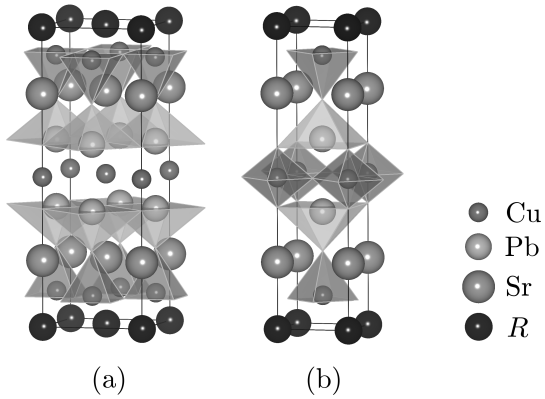

Figure 16. The crystal structures of (a) $Pb_2CuSr_2RCu_2O_8$ and (b) $Pb_2CuSr_2RCu_2O_{10}$. The light and dark grey polyhedra represent the oxygen coordination of Pb and Cu, respectively. Oxygen atoms are located at corners of the polyhedra.

6.2 Oxygen Absorption/Desorption Behaviour

The thermal behaviours of $Pb_2CuSr_2RCu_2O_{8+\delta}$ and $YBaCo_4O_{7+\delta}$ in oxygen atmosphere are similar with a rapid low-temperature absorption of oxygen at about 200-300 °C followed by a rapid desorption at higher temperature as shown in Figure 17. Compared with the prototype cuprate superconductor $CuBa_2YCu_2O_{6+\delta}$, with a slow gradual desorption of the absorbed oxygen, both of these compounds have significantly different thermal behaviours. In general the gradual desorption of oxygen is more common for oxides than the rapid desorption in a single distinguishable step seen for $YBaCo_4O_{7+\delta}$ and $Pb_2CuSr_2RCu_2O_{8+\delta}$.

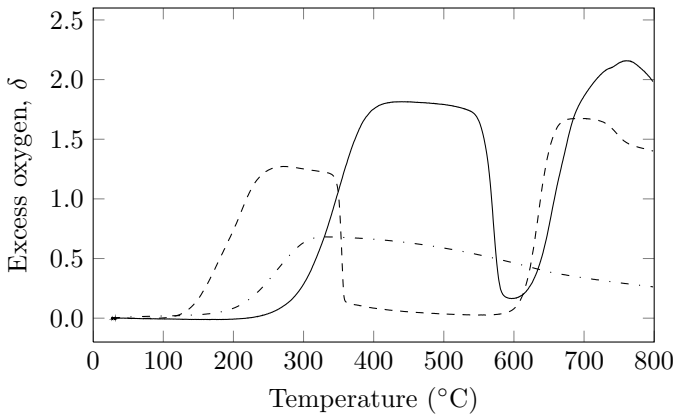

Figure 17. Dependence of oxygen content of $Pb_2CuSr_2NdCu_2O_{8+\delta}$ (——), $YBaCo_4O_{7+\delta}$ (- - -) and $CuBa_2YCu_2O_{6+\delta}$ (- · -) on temperature.

The thermal behaviour of $Pb_2CuSr_2RCu_2O_{8+\delta}$ can be summarised by determining the absorption, desorption and decomposition temperatures (Figure 18) from maximum points of the derivative curves, $\Delta m/\Delta T$, from thermogravimetric measurements.

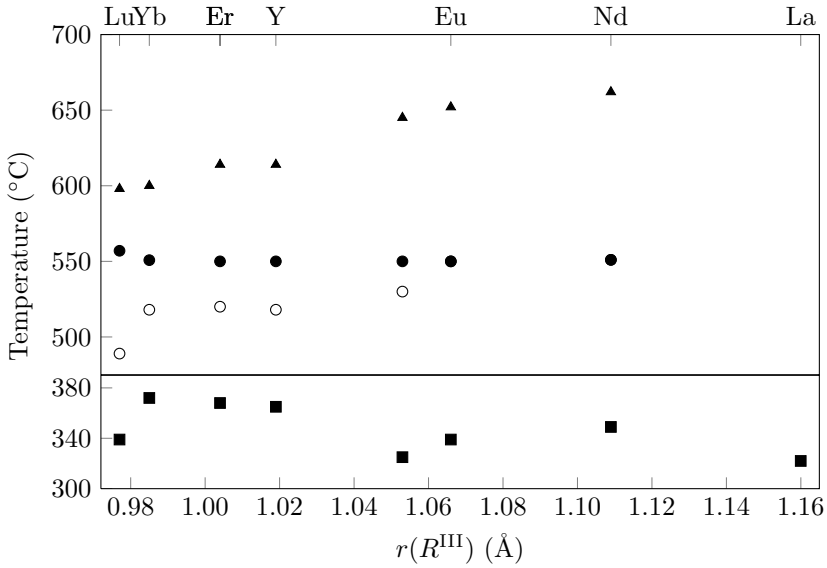

Figure 18. Temperatures of oxygen absorption (■), first step of desorption (○), second step of desorption (●) and decomposition (▲) as a function of ionic radius, $r(R^{III})$, of the rare-earth constituent in $Pb_2CuSr_2RCu_2O_{8+\delta}$.

The relatively rapid absorption of oxygen $Pb_2CuSr_2RCu_2O_{8+\delta}$ starts at fairly low temperature of about 250 °C decreasing as the size of R increases. This kind of behaviour is to be expected as the introduction of larger atoms to the lattice causes the expansion of the lattice in all directions resulting in an easier absorption of oxygen. Although the initial absorption temperature is higher than that of $YBaCo_4O_{7+\delta}$,[133] it still is low enough for many applications and it extends the temperature range of such materials as $YBaCo_4O_{7+\delta}$ is only useful at lower temperatures. The amount of absorbed oxygen is also important when considering the usefulness of a compound for practical applications. For oxygen-storage applications this is defined as oxygen-storage capacity (OSC) usually expressed in units of μmol (O)/g (material). In the dynamic thermogravimetric measurements of $Pb_2CuSr_2RCu_2O_{8+\delta}$ the amount of absorbed oxygen, δ, increases from 1.6 up to 2.0 with the increasing size of R although in isothermal measurements at the temperature of the maximal absorption the amount of absorbed oxygen can be increased closer to 2 even in the compounds with the smallest R. Eventhough

the amount of absorbed oxygen of the compounds with the smallest R obtainable in isothermal measurements is larger than that in dynamic measurements, the practically available range of oxygen non-stoichiometry is closer to that seen in dynamic thermogravimetric measurements. The maximum oxygen absorption of $\delta \approx 2$ corresponds to an OSC value of 1900 μmol−O/g which is somewhat higher than the 1500 μmol−O/g for the commercial CeO_2−ZrO_2[148] oxygen storage material but not as high as the values of 2700 μmol−O/g and 2500 μmol−O/g for $YBaCo_4O_{7+\delta}$[133,134] and CeO_2−CrO_2,[149] respectively.

In the case of smaller R oxygen desorption occurs in two distinct steps whereas for larger R desorption happens in a single step. The temperature of the latter desorption step is essentially identical with desorption temperatures for larger R. Since the lattice expansion has no influence on the onset temperature of oxygen desorption is probably purely thermally induced. Contrary to compounds with other R, $Pb_2CuSr_2LaCu_2O_{8+\delta}$ does not undergo desorption of oxygen before decomposition.

6.3 Thermal Stability

The decomposition of $Pb_2CuSr_2RCu_2O_{8+\delta}$ at a relatively low temperature in air is a disadvantage for possible applications, which is also true for $YBaCo_4O_{7+\delta}$.[133] The latter, however, can be made stable also at high temperatures by careful selection of substituents on the Co sites[135,137,150] although it is difficult to both stabilise the structure at high temperatures and retain the desired low temperature oxygen absorption properties as the substituents necessary for stabilisation are usually not as easily oxidised and reduced. However in $YBaCo_4O_7$ the Co atoms are already in mixed valence state (Co^{2+}/Co^{3+}) and therefore the substitution of Co with trivalent cations does not necessarily have any significant effect on the oxygen absorption properties as has been observed in case of Al and Ga substitutions where reasonable absorption properties are retained.[135,150]

In $Pb_2CuSr_2RCu_2O_{8+\delta}$ the decomposition temperature increases as the size of R increases with the exception of La which decomposes at a significantly lower temperature and no desorption step is observed before the compound decomposes. The lower decomposition temperature of $Pb_2CuSr_2LaCu_2O_{8+\delta}$ may be caused by increasing mixing of atoms between the Sr and R sites due to more similar ionic radii of Sr and La. Therefore the preference of the larger Sr to a higher coordination number on R site may be causing an undesired octahedral coordination of Cu instead of square-planar coordination resulting in

decomposition at lower temperature.

Even though the $Pb_2CuSr_2RCu_2O_{8+\delta}$ structure could not be stabilised at high temperatures for any of the R constituents, the possibility of stabilisation at high temperature still exists although not for certain. In $Pb_2CuSr_2RCu_2O_{8+\delta}$ substitution of Cu with other transition metals or similar elements might be possible but may not be as easy as in $YBaCo_4O_{7+\delta}$ due to the coordination of Cu atoms in two quite different crystallographic sites in different valence states requiring careful selection of the substituents.

7 CONCLUSIONS

Understanding the factors affecting the physical properties as well as thermal and chemical stability is crucially important when designing new functional materials for future applications. In this thesis, the synthesis and characterisation of new double-perovskite oxides and related layered compounds, and the redox chemistry and stability of perovskite-related layered compounds were described.

Through the substitutions of *B*-site cations in $Sr_2MgMoO_{6-\delta}$ with various transition metals it was possible to control the crystal structure, electrical conductivity and thermal stability. Thermal stability was significantly decreased after a complete substitution of Mg with nominally divalent first-row transition-metal atoms. The tendency of some transition metals to exhibit mixed valence in oxides was found to depress cation ordering. Substitution of Mo with either Nb or W did not significantly affect the thermal stability of the compound but decreased both the reducibility and electrical conductivity compared with the parent phase. In the case of niobium substitution, the effect on reducibility was more significant due to intrinsic oxygen vacancies introduced to the structure preventing further formation of oxygen vacancies.

During the course of the search for new Ruddlesden–Popper derivatives of the $Sr_2MgMoO_{6-\delta}$-type double perovskites, a series of novel $n = 2$ RP compounds $(Sr_{1-x}La_x)_3(Mg_{1/3+x/2}Nb_{2/3-x/2})_2O_7$ $(0.15 \leq x \leq 0.33)$ was discovered. The characterisation of the compounds with XRD and ED clearly indicated at least partial *B*-site ordering, not very common for the structural type. The compounds, however, were observed not to exhibit significant amounts of oxygen vacancies in reducing conditions.

Many layered perovskite-derived Ruddlesden–Popper-type compounds have been found to topotactically react with water forming a crystalline derivative phase even in ambient conditions. In addition to the possible applications of the derivative phases, the stability of the parent RP compounds is of great importance in terms of applications. In this thesis a comprehensive study of factors influencing the reactivity of the RP compounds was presented indicating that both elemental composition and oxygen content are important factors when determining whether a derivative can be formed.

Following the recent discovery of the interesting new oxygen storage material $YBaCo_4O_{7+\delta}$ and the increasing interest in cleaner energy the perovskite-derived $Pb_2CuSr_2RCu_2O_{8+\delta}$ was revisited. The effect of the rare-earth substituent R on the reversible low-temperature oxygen-storage capacity and thermal stability of $Pb_2CuSr_2RCu_2O_{8+\delta}$ was investigated. The oxygen-absorption capability was found to increase with increasing ionic radius of R whereas the desorption was essentially unaffected. Similarly, the decomposition temperature was also increased with increasing ionic radius of R but it was not, however, possible to completely prevent the decomposition solely by the selection of the rare-earth constituent.

REFERENCES

1. Bednorz, J. G. and Müller, K. A. *Z. Phys. B Con. Mat.* **64**, 189–193 (1986).

2. von Helmolt, R., Wecker, J., Holzapfel, B., Schultz, L., and Samwer, K. *Phys. Rev. Lett.* **71**, 2331–2333 (1993).

3. von Helmolt, R., Wecker, J., Samwer, K., Haupt, L., and Barner, K. *J. Appl. Phys.* **76**, 6925–6928 (1994).

4. Hwang, H. Y., Cheong, S.-W., Radaelli, P. G., Marezio, M., and Batlogg, B. *Phys. Rev. Lett.* **75**, 914–917 (1995).

5. Kobayashi, K.-I., Kimura, T., Sawada, H., Terakura, K., and Tokura, Y. *Nature* **395**, 677–680 (1998).

6. Kimura, T., Goto, T., Shintani, H., Ishizaka, K., Arima, T., and Tokura, Y. *Nature* **426**, 55–58 (2003).

7. Trovarelli, A., de Leitenburg, C., Boaro, M., and Dolcetti, G. *Catal. Today* **50**, 353–367 (1999).

8. Kašpar, J., Fornasiero, P., and Hickey, N. *Catal. Today* **77**, 419–449 (2003).

9. Zhang, K., Zhu, Z., Ran, R., Shao, Z., Jin, W., and Liu, S. *J. Alloys Compd.* **492**, 552–558 (2010).

10. Rui, Z., Ding, J., Fang, L., Lin, Y., and Li, Y. *Fuel* **94**, 191–196 (2012).

11. Anderson, M. T., Greenwood, K. B., Taylor, G. A., and Poeppelmeier, K. R. *Prog. Solid State Chem.* **22**, 197–233 (1993).

12. Woodward, P., Hoffmann, R.-D., and Sleight, A. *J. Mater. Res.* **9**, 2118–2127 (1994).

13. Wu, M. K., Ashburn, J. R., Torng, C. J., Hor, P. H., Meng, R. L., Gao, L., Huang, Z. J., Wang, Y. Q., and Chu, C. W. *Phys. Rev. Lett.* **58**, 908–910 (1987).

14. Dion, M., Ganne, M., and Tournoux, M. *Mater. Res. Bull.* **16**, 1429–1435 (1981).

15. Jacobson, A. J., Johnson, J. W., and Lewandowski, J. T. *Inorg. Chem.* **24**, 3727–3729 (1985).

16. Jacobson, A., Lewandowski, J., and Johnson, J. W. *J. Less-Common Met.* **116**, 137–146 (1986).

17. Ruddlesden, S. N. and Popper, P. *Acta Crystallogr.* **10**, 538–539 (1957).

18. Ruddlesden, S. N. and Popper, P. *Acta Crystallogr.* **11**, 54–55 (1958).

19. Aurivillius, B. *Ark. Kemi* **1**, 499–512 (1949).

20. Grigoraviciute, I., Karppinen, M., Chan, T.-S., Liu, R.-S., Chen, J.-M., Chmaissem, O., and Yamauchi, H. *J. Am. Chem. Soc.* **132**, 838–841 (2010). PMID: 20017548.

21. Chmaissem, O., Grigoraviciute, I., Yamauchi, H., Karppinen, M., and Marezio, M. *Phys. Rev. B* **82**, 104507 (2010).

22. Gao, W., Oishi, K., Suematsu, H., Yamauchi, H., and Karppinen, M. *Solid State Commun.* **151**, 1400–1403 (2011).

23. Jorgensen, J. D., Dabrowski, B., Pei, S., Hinks, D. G., Soderholm, L., Morosin, B., Schirber, J. E., Venturini, E. L., and Ginley, D. S. *Phys. Rev. B* **38**, 11337–11345 (1988).

24. Jorgensen, J. D., Dabrowski, B., Pei, S., Richards, D. R., and Hinks, D. G. *Phys. Rev. B* **40**, 2187–2199 (1989).

25. Takada, K., Sakurai, H., Takayama-Muromachi, E., Izumi, F., Dilanian, R. A., and Sasaki, T. *Nature* **422**, 53–55 (2003).

26. Gopalakrishnan, J., Sivakumar, T., Thangadurai, V., and Subbanna, G. N. *Inorg. Chem.* **38**, 2802–2806 (1999).

27. Yokokawa, H., Tu, H., Iwanschitz, B., and Mai, A. *J. Power Sources* **182**, 400–412 (2008).

28. Robin, M. B. and Day, P. Mixed valence chemistry–a survey and classification. volume 10 of *Advances in Inorganic Chemistry and Radiochemistry*, 247–422. Academic Press (1968).

29. Birgeneau, R., Aharony, A., Belk, N., Chou, F., Endoh, Y., Greven, M., Hosoya, S., Kastner, M., Lee, C., Lee, Y., Shirane, G., Wakimoto, S., Wells, B., and Yamada, K. *J. Phys. Chem. Solids* **56**, 1913–1919 (1995). ¡ce:title¿Proceedings of the Conference on Spectroscopies in Novel Superconductors¡/ce:title¿.

30. Takeda, Y., Kanno, K., Takada, T., Yamamoto, O., Takano, M., Nakayama, N., and Bando, Y. *J. Solid State Chem.* **63**, 237–249 (1986).

31. Hodges, J. P., Short, S., Jorgensen, J. D., X., X., Dabrowski, B., Mini, S. M., and Kimball, C. W. *J. Solid State Chem.* **151**, 190–209 (2000).

32. Marezio, M., Bordet, P., Capponi, J. J., Cava, R. J., Chaillout, C., Chenavas, J., Hewat, A. W., Hewat, E. A., Hodeau, J. L., and Strobel, P. *Physica C* **162–164**, 281–284 (1989).

33. Marezio, M. *Acta Cryst.* **A47**, 640–654 (1991).

34. Tofield, B. and Scott, W. *J. Solid State Chem.* **10**, 183–194 (1974).

35. Van Roosmalen, J., Cordfunke, E., Helmholdt, R., and Zandbergen, H. *J. Solid State Chem.* **110**, 100–105 (1994).

36. Mitchell, J. F., Argyriou, D. N., Potter, C. D., Hinks, D. G., Jorgensen, J. D., and Bader, S. D. *Phys. Rev. B* **54**, 6172–6183 (1996).

37. Alonso, J. A., Martinez-Lope, M. J., Casais, M. T., Macmanus-Driscoll, J. L., de Silva, P. S. I. P. N., Cohen, L. F., and Fernandez-Diaz, M. T. *J. Mater. Chem.* **7**, 2139–2144 (1997).

38. Huang, Q., Santoro, A., Lynn, J. W., Erwin, R. W., Borchers, J. A., Peng, J. L., and Greene, R. L. *Phys. Rev. B* **55**, 14987–14999 (1997).

39. Thomas, D. *J. Phys. Chem. Solids* **3**, 229–237 (1957).

40. Hutson, A. R. *Phys. Rev.* **108**, 222–230 (1957).

41. Goodenough, J. B. *Annu. Rev. Mater. Res.* **33**, 91–128 (2003).

42. Carter, S., Selcuk, A., Chater, R., Kajda, J., Kilner, J., and Steele, B. *Solid State Ionics* **53–56**, 597–605 (1992).

43. Minh, N. Q. *J. Am. Ceram. Soc.* **76**, 563–588 (1993).

44. Maguire, E., Gharbage, B., Marques, F. M. B., and Labrincha, J. A. *Solid State Ionics* **127**, 329–335 (2000).

45. Tarancón, A., Morata, A., Dezanneau, G., Skinner, S. J., Kilner, J. A., Estradé, S., Hernández-Ramírez, F., Peiró, F., and Morante, J. *J. Power Sources* **174**, 255–263 (2007).

46. Kim, J.-H. and Manthiram, A. *J. Electrochem. Soc.* **155**, B385–B390 (2008).

47. Zhou, Q., He, T., and Ji, Y. *J. Power Sources* **185**, 754–758 (2008).

48. Fergus, J. W. *J. Power Sources* **162**, 30–40 (2006).

49. Wachsman, E. D. and Lee, K. T. *Science* **334**, 935–939 (2011).

50. Ishihara, T., Matsuda, H., and Takita, Y. *J. Am. Chem. Soc.* **116**, 3801–3803 (1994).

51. Ishihara, T., Matsuda, H., and Takita, Y. *Solid State Ionics* **79**, 147–151 (1995).

52. Huang, P. and Petric, A. *J. Electrochem. Soc.* **143**, 1644–1648 (1996).

53. Huang, K., Tichy, R. S., and Goodenough, J. B. *J. Am. Ceram. Soc.* **81**, 2565–2575 (1998).

54. Huang, Y.-H., Dass, R. I., Denyszyn, J. C., and Goodenough, J. B. *J. Electrochem. Soc.* **153**, 1266–1272 (2006).

55. Huang, Y.-H., Dass, R. I., Xing, Z.-L., and Goodenough, J. B. *Science* **312**, 254–257 (2006).

56. Ji, Y., Huang, Y.-H., Ying, J.-R., and Goodenough, J. B. *Electrochem. Commun.* **9**, 1881–1885 (2007).

57. Zhang, L. and He, T. *J. Power Sources* **196**, 8352–8359 (2011).

58. Matsuda, Y., Karppinen, M., Yamazaki, Y., and Yamauchi, H. *J. Solid State Chem.* **182**, 1713–1716 (2009).

59. Williams, E. J. *Proc. R. Soc. Lond. A* **152**, 231–252 (1935).

60. Bernuy-Lopez, C., Allix, M., Bridges, C., Claridge, J., and Rosseinsky, M. *Chem. Mater.* **19**, 1035–1043 (2007).

61. Shannon, R. D. *Acta Cryst.* **A32**, 751–767 (1976).

62. Wei, T., Ji, Y., Meng, X., and Zhang, Y. *Electrochem. Commun.* **10**, 1369–1372 (2008).

63. Mott, N. F. and Davis, E. A. *Electronic processes in non-crystalline materials.* Clarendon Press, Oxford University Press, Oxford, New York, 2nd edition, (1979).

64. Zhang, P., Huang, Y.-H., Cheng, J.-G., Mao, Z.-Q., and Goodenough, J. B. *J. Power Sources* **196**, 1738–1743 (2011).

65. Xie, Z., Zhao, H., Du, Z., Chen, T., Chen, N., Liu, X., and Skinner, S. J. *J. Phys. Chem. C* **116**, 9734–9743 (2012).

66. Wang, Z., Tian, Y., and Li, Y. *J. Power Sources* **196**, 6104–6109 (2011).

67. Xie, Z., Zhao, H., Chen, T., Zhou, X., and Du, Z. *Int. J. Hydrogen Energy* **36**, 7257–7264 (2011).

68. Zhang, Q., Wei, T., and Huang, Y.-H. *J. Power Sources* **198**, 59–65 (2012).

69. Escudero, M., Aguadero, A., Alonso, J., and Daza, L. *J. Electroanal. Chem.* **611**, 107–116 (2007).

70. Tsipis, E. and Kharton, V. *J. Solid State Electrochem.* **15**, 1007–1040 (2011).

71. Rodriguez-Carvajal, J., Fernandez-Diaz, M. T., and Martinez, J. L. *J. Phys.: Condens. Matter* **3**, 3215 (1991).

72. Rice, D. and Buttrey, D. *J. Solid State Chem.* **105**, 197–210 (1993).

73. Paulus, W., Cousson, A., Dhalenne, G., Berthon, J., Revcolevschi, A., Hosoya, S., Treutmann, W., Heger, G., and Toquin, R. L. *Solid State Sci.* **4**, 565–573 (2002).

74. Amow, G. and Skinner, S. *J. Solid State Electrochem.* **10**, 538–546 (2006).

75. Bernuy-Lopez, C., Pelloquin, D., Raveau, B., Allix, M., Claridge, J. B., Rosseinsky, M. J., Wang, P., and Bleloch, A. *Solid State Ionics* **181**, 889–893 (2010).

76. Dann, S. E., Weller, M. T., and Currie, D. B. *J. Solid State Chem.* **97**, 179–185 (1992).

77. Demazeau, G., Oh-Kim, E. O., Wang, K. T., Fournes, L., Dance, J. M., Pouchard, M., and Hagenmuller, P. *Rev. Chim. Miner.* **24**, 183–189 (1987).

78. Warda, S. A., Massa, W., Reinen, D., Hu, Z., Kaindl, G., and de Groot, F. M. *J. Solid State Chem.* **146**, 79–87 (1999).

79. Burley, J. C., Battle, P. D., Gallon, D. J., Sloan, J., Grey, C. P., and Rosseinsky, M. J. *J. Am. Chem. Soc.* **124**, 620–628 (2002).

80. Battle, P. D., Burley, J. C., Gallon, D. J., Grey, C. P., and Sloan, J. *J. Solid State Chem.* **177**, 119–125 (2004).

81. Heap, R., Islam, M. S., and Slater, P. R. *Dalton Trans.* , 460–463 (2005).

82. Rodgers, J. A., Battle, P. D., Dupré, N., Grey, C. P., and Sloan, J. *Chem. Mater.* **16**, 4257–4266 (2004).

83. Rodgers, J. A., Battle, P. D., Grey, C. P., and Sloan, J. *Chem. Mater.* **17**, 4362–4373 (2005).

84. Battle, P. D., Grey, C. P., Rodgers, J. A., and Sloan, J. *Solid State Sci.* **8**, 280–288 (2006).

85. Hosomi, T., Suematsu, H., Fjellvåg, H., Karppinen, M., and Yamauchi, H. *J. Mater. Chem.* **9**, 1141–1148 (1999).

86. Karppinen, M., Yamauchi, H., Hosomi, T., Suematsu, H., and Fjellvåg, H. *J. Low Temp. Phys.* **117**, 843–847 (1999).

87. Yamauchi, H., Karppinen, M., Hosomi, T., and Fjellvåg, H. *Physica C* **338**, 38–45 (2000).

88. Karppinen, M., Hosomi, T., and Yamauchi, H. *Physica C* **382**, 276–282 (2002).

89. Yamauchi, H., Karppinen, M., Hosomi, T., and Suematsu, H. *Physica C* **338**, 46–51 (2000).

90. Takata, T., Shinohara, K., Tanaka, A., Hara, M., Kondo, J., and Domen, K. *J. Photochem. Photobiol. A* **106**, 45–49 (1997).

91. Takata, T., Furumi, Y., Shinohara, K., Tanaka, A., Hara, M., Kondo, J. N., and Domen, K. *Chem. Mater.* **9**, 1063–1064 (1997).

92. Shimizu, K., Tsuji, Y., Kawakami, M., Toda, K., Kodama, T., Sato, M., and Kitayama, Y. *Chem. Lett.* **31**, 1158–1159 (2002).

93. Reddy, V. R., Hwang, D. W., and Lee, J. S. *Catal. Lett.* **90**, 39–43 (2003).

94. Shimizu, K., Tsuji, Y., Hatamachi, T., Toda, K., Kodama, T., Sato, M., and Kitayama, Y. *Phys. Chem. Chem. Phys.* **6**, 1064–1069 (2004).

95. Shimizu, K., Itoh, S., Hatamachi, T., Kodama, T., Sato, M., and Toda, K. *Chem. Mater.* **17**, 5161–5166 (2005).

96. Yao, W. and Ye, J. *Chem. Phys. Lett.* **435**, 96–99 (2007).

97. Machida, M., Murakami, H., Kitsubayashi, T., and Kijima, T. *J. Chem. Soc., Chem. Commun.* , 485–486 (1995).

98. Machida, M., Murakami, H., Kitsubayashi, T., and Kijima, T. *Chem. Mater.* **8**, 197–203 (1996).

99. Machida, M., Masuda, N., and Kijima, T. *J. Mater. Chem.* **9**, 1369–1374 (1999).

100. Nishi, T., Toda, K., Kanamaru, F., and Sakai, T. *Key Eng. Mater.* **169–170**, 235–238 (1999).

101. Pelloquin, D., Hadermann, J., Giot, M., Caignaert, V., Michel, C., Hervieu, M., and Raveau, B. *Chem. Mater.* **16**, 1715–1724 (2004).

102. Jantsky, L., Okamoto, H., Demont, A., and Fjellvåg, H. *Inorg. Chem.* **51**, 9181–9191 (2012).

103. Motohashi, T., Raveau, B., Caignaert, V., Pralong, V., Hervieu, M., Pelloquin, D., and Maignan, A. *Chem. Mater.* **17**, 6256–6262 (2005).

104. Pelloquin, D., Barrier, N., Flahaut, D., Caignaert, V., and Maignan, A. *Chem. Mater.* **17**, 773–780 (2005).

105. Bréard, Y., Raveau, B., Pelloquin, D., and Maignan, A. *J. Mater. Chem.* **17**, 2818–2823 (2007).

106. Pelloquin, D., Barrier, N., Maignan, A., and Caignaert, V. *Solid State Sci.* **7**, 853–860 (2005).

107. Baszczuk, A. *J. Alloys Compd.* **414**, 287–292 (2006).

108. Toda, K., Kameo, Y., Kurita, S., and Sato, M. *Bull. Chem. Soc. Jpn.* **69**, 349–352 (1996).

109. Nishimoto, S., Matsuda, M., and Miyake, M. *J. Solid State Chem.* **178**, 811–818 (2005).

110. Chen, D., Jiao, X., and Xu, R. *Mater. Res. Bull.* **34**, 685–691 (1999).

111. Schaak, R. E. and Mallouk, T. E. *J. Solid State Chem.* **161**, 225–232 (2001).

112. Gopalakrishnan, J. and Bhat, V. *Inorg. Chem.* **26**, 4299–4301 (1987).

113. Richard, M., Brohan, L., and Tournoux, M. *J. Solid State Chem.* **112**, 345–354 (1994).

114. Toda, K., Watanabe, J., and Sato, M. *Mater. Res. Bull.* **31**, 1427–1435 (1996).

115. Schaak, R. E. and Mallouk, T. E. *J. Am. Chem. Soc.* **122**, 2798–2803 (2000).

116. Byeon, S.-H. and Nam, H.-J. *Chem. Mater.* **12**, 1771–1778 (2000).

117. Kodenkandath, T. A. and Wiley, J. B. *Mater. Res. Bull.* **35**, 1737–1742 (2000).

118. Crosnier-Lopez, M.-P., Berre, F. L., and Fourquet, J.-L. *J. Mater. Chem.* **11**, 1146–1151 (2001).

119. Crosnier-Lopez, M. P., Le Berre, F., and Fourquet, J. L. *Z. Anorg. Allg. Chem.* **628**, 2049–2056 (2002).

120. Le Berre, F., Crosnier-Lopez, M. P., Laligant, Y., and Fourquet, J. L. *J. Mater. Chem.* **12**, 258–263 (2002).

121. Schaak, R. E. and Mallouk, T. E. *J. Solid State Chem.* **155**, 46–54 (2000).

122. Shpanchenko, R., Antinov, E., and Kovba, L. *Mater. Sci. Forum* **133–136**, 639–644 (1993).

123. Minichelli, D. and Longo, V. *J. Mater. Sci.* **13**, 2069–2070 (1978).

124. Gallagher, P. K., MacChesney, J. B., and Buchanan, D. N. E. *J. Chem. Phys.* **45**, 2466–2471 (1966).

125. Nevskii, N. N., Ivanov-Emin, B. N., Nevskaya, N. A., Kaziev, G. Z., and Belov, N. V. *Dokl. Akad. Nauk SSSR* **264**, 857–858 (1982).

126. Toda, K., Kameo, Y., Fujimoto, M., and Sato, M. *J. Ceram. Soc. Jpn.* **102**, 737–741 (1994).

127. Toda, K., Kameo, Y., Ohta, M., and Sato, M. *J. Alloys Compd.* **218**, 228–232 (1995).

128. Sato, M., Jin, T., and Ueda, H. *Chem. Lett.* **23**, 161–164 (1994).

129. Bhuvanesh, N. S. P., Crosnier-Lopez, M. P., Duroy, H., and Fourquet, J. L. *J. Mater. Chem.* **9**, 3093–3100 (1999).

130. Xu, Z., Qi, Z., and Kaufman, A. *J. Power Sources* **115**, 40–43 (2003).

131. Kodama, T. and Gokon, N. *Chem. Rev.* **107**, 4048–4077 (2007).

132. Sakakini, B., Taufiq-Yap, Y., and Waugh, K. *J. Catal.* **189**, 253–262 (2000).

133. Karppinen, M., Yamauchi, H., Otani, S., Fujita, T., Motohashi, T., Huang, Y.-H., Valkeapaa, M., and Fjellvag, H. *Chem. Mater.* **18**, 490–494 (2006).

134. Räsänen, S., Yamauchi, H., and Karppinen, M. *Chem. Lett.* **37**, 638–639 (2008).

135. Räsänen, S., Motohashi, T., Yamauchi, H., and Karppinen, M. *J. Solid State Chem.* **183**, 692–695 (2010).

136. Komiyama, T., Motohashi, T., Masubuchi, Y., and Kikkawa, S. *Mater. Res. Bull.* **45**, 1527–1532 (2010).

137. Räsänen, S., Parkkima, O., Rautama, E.-L., Yamauchi, H., and Karppinen, M. *Solid State Ionics* **208**, 31–35 (2012).

138. Zhang, S., Song, H., Jia, J., Yang, D., Sun, H., and Hu, X. *Ceram.-Silikaty* **55**, 195–197 (2011).

139. Kim, Y., Kim, J.-H., and Manthiram, A. *Int. J. Hydrogen Energy* **36**, 15295–15303 (2011).

140. Tsipis, E. V., Kharton, V. V., Frade, J. R., and Núñez, P. *J. Solid State Electrochem.* **9**, 547–557 (2005).

141. Tsipis, E. V., Kharton, V. V., and Frade, J. R. *Solid State Ionics* **177**, 1823–1826 (2006).

142. Cava, R. J., Batlogg, B., Krajewski, J. J., Rupp, L. W., Schneemeyer, L. F., Siegrist, T., vanDover, R. B., Marsh, P., Peck Jr, W. F., Gallagher, P. K., Glarum, S. H., Marshall, J. H., Farrow, R. C., Waszczak, J. V., Hull, R., and Trevor, P. *Nature* **336**, 211–214 (1988).

143. Fujishita, H., Yamagata, S.-i., and Sato, M. *J. Phys. Soc. Jpn.* **60**, 913–920 (1991).

144. Mochiku, T. and Kadowaki, K. *J. Phys. Soc. Jpn.* **61**, 881–890 (1992).

145. Yamaguchi, H., Oyanagi, H., Tokiwa, A., and Syono, Y. *Physica C* **185-189**, 853–854 (1991).

146. Karppinen, M., Fukuoka, A., Wang, J., Takano, S., Wakata, M., Ikemachi, T., and Yamauchi, H. *Physica C* **208**, 130–136 (1993).

147. Karppinen, M., Kotiranta, M., Yamauchi, H., Nachimuthu, P., Liu, R. S., and Chen, J. M. *Phys. Rev. B* **63**, 184507 (2001).

148. Nagai, Y., Yamamoto, T., Tanaka, T., Yoshida, S., Nonaka, T., Okamoto, T., Suda, A., and Sugiura, M. *Catal. Today* **74**, 225–234 (2002).

149. Singh, R., Sharma, T., Singh, A., Anindita, Mishra, D., and Tiwari, S. *Electrochim. Acta* **53**, 2322–2330 (2008).

150. Parkkima, O., Yamauchi, H., and Karppinen, M. *Chem. Mater.* **25**, 599–604 (2013).